Science of the Total Environment 891 (2023) 164357

Contents lists available at ScienceDirect

Science of the Total Environment

journal homepage: www.elsevier.com/locate/scitotenv

Sea spray as a secondary source of chlorinated persistent organic pollutants? - Conclusions from a comparison of seven fresh snowfall events in 2019 and 2021

Filip Pawlak [a,1], Krystyna Koziol [b,1,*], Marcin Frankowski [c], Łukasz Nowicki [e], Christelle Marlin [f], Anna Maria Sulej-Suchomska [d], Żaneta Polkowska [a,*]

[a] Department of Analytical Chemistry, Faculty of Chemistry, Gdansk University of Technology, 11/12 Narutowicza St., Gdańsk 80-233, Poland
[b] Faculty of Geographical Sciences, Kazimierz Wielki University, 8 Koscielecki Sq., Bydgoszcz 85-033, Poland
[c] Department of Analytical and Environmental Chemistry, Faculty of Chemistry, Adam Mickiewicz University in Poznan, Uniwersytetu Poznańskiego 8, 61-614 Poznań, Poland
[d] Department of Quality Management, Faculty of Management and Quality Sciences, Gdynia Maritime University, 81-225 Gdynia, Poland
[e] Perlan Technologies Poland Ltd., the Pomeranian Science and Technology Park, aleja Zwycięstwa 96/98, 81-451 Gdynia, Poland
[f] University Paris-Saclay, Université Paris-Sud 11, Orsay, Île-de-France, France

HIGHLIGHTS

- Fresh snow and seawater microlayer sampled for chlorinated POPs concentrations
- Two years of spring Arctic snowfall showed vastly different Cl-POPs concentrations.
- 2019 impacted by long-range transport (LRT) while 2021 showed mainly local factors.
- POPs compounds enriched in seawater microlayer were predominant in 2021 snow.
- Sea spray transports Cl-POPs inland in the Arctic, yet LRT dominates Cl-POP fluxes.

GRAPHICAL ABSTRACT

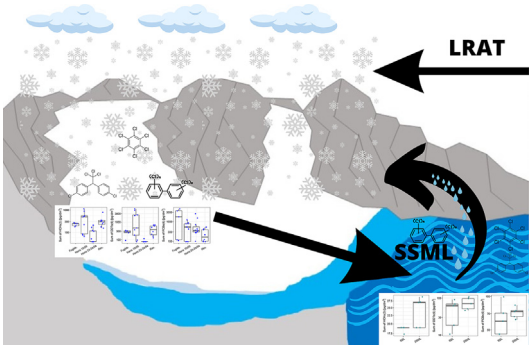

ARTICLE INFO

Editor: Hai Guo

Keywords:
OCPs
PCBs
Snow
Marine aerosol
Arctic
Atmospheric transport

ABSTRACT

Secondary sources of persistent organic pollutants (POPs) gain in importance worldwide as primary sources decline. In this work, we aim to determine whether sea spray may be a secondary source of chlorinated POPs to the terrestrial Arctic, since a similar mechanism was proposed there only for the more water-soluble POPs. To this end, we have determined polychlorinated biphenyls and organochlorine pesticides concentrations in fresh snow and seawater collected in the vicinity of the Polish Polar Station in Hornsund in two sampling periods covering spring 2019 and 2021. To support our interpretations, we include also metal and metalloid, and stable hydrogen and oxygen isotopes analysis in those samples. A significant correlation was found between the concentrations of POPs and the distance from the sea at the sampling point, yet the confirmation of sea spray impact lies more in capturing an event with negligible long-range transport influence where the detected chlorinated POPs (Cl-POPs) matched in composition the compounds enriched in the sea surface microlayer, which is both a source of sea spray and a seawater microenvironment rich in hydrophobic substances.

Abbreviations: OCPs, organochlorine pesticides; PCBs, polychlorinated biphenyls.

* Corresponding authors.
E-mail addresses: krystyna.koziol@ukw.edu.pl (K. Koziol), zanpolko@pg.edu.pl (Ż. Polkowska).

[1] Both first authors had equal contribution to the article.

http://dx.doi.org/10.1016/j.scitotenv.2023.164357
Received 28 February 2023; Received in revised form 5 May 2023; Accepted 18 May 2023
Available online 20 May 2023

1. Introduction

Secondary sources of pollution, especially persistent organic pollutants (POPs), are an increasingly recognised concern in the Arctic (Ademollo et al., 2021; Carlsson et al., 2016; Kallenborn et al., 2011; Ma et al., 2011; Pawlak et al., 2021; Pouch et al., 2021b). It has been strongly established that melting glaciers may act as secondary sources of POPs in the Arctic (Ademollo et al., 2021; Pawlak et al., 2021; Pouch et al., 2021b). Other potential secondary sources, discussed and evidenced in the literature, are permafrost thaw (Kosek et al., 2019; McGovern et al., 2022; Muir and Galarneau, 2021), revolatilisation from the seawater (Ma et al., 2016, 2011) and soils (Cabrerizo et al., 2018; Ma et al., 2011), as well as the revolatilisation and melting of snow (short-term storage; Hansen et al., 2014; McGovern et al., 2022; Pawlak et al., 2021). In this article, we test the hypothesis formulated based on the published literature, that another secondary source of legacy POPs in the terrestrial Arctic may be the sea spray dispersal.

In the global scheme of pollutant fate, the ocean is usually considered the final sink, yet at the regional and local scale it may become a secondary source. Stemmler and Lammel (2013) demonstrate that ocean currents deliver chlorinated POPs (Cl-POPs) such as polychlorinated biphenyls (PCBs) and dichlorodiphenyltrichloroethane (DDT) into the Arctic. These are carried especially in the East Greenland and Labrador Currents, yet the general concentration of PCBs and DDTs in the Arctic surface waters is higher than in the low latitudes. Such elevated seawater concentration may result in POPs revolatilisation into the atmosphere, as was shown for DDT by Stemmler and Lammel (2009), especially since the removal into sediment is slow (only up to 5.5 % of sea-borne DDT has been removed into sediment to date), the sea surface temperature rises and sea ice cover decreases. This effect was already observed in the pollution trends by Ma et al. (2011), and not only for the highly volatile compounds, such as the α-HCH (Wong et al., 2011). It has also been predicted that the net flux of POPs between the Arctic and lower latitudes will shift in the future, depending on the pollutant type and properties, with e.g. DDT to be imported more efficiently and e.g. PCB-153 to be exported more intensively (Octaviani et al., 2015). Therefore, a better understanding of POPs fate in the Arctic may help us understand its impact on the global pollution distribution in the future.

Whilst the volatilisation flux of gaseous Cl-POPs has been described in detail in the Arctic (Jantunen et al., 2015), the observations related to less volatile compounds suggest a second mechanism or pollutant release from the sea surface may be also playing a role (Ma et al., 2011), connected to the production of aerosol by wind action and wave breaking (Nilsson et al., 2001; van Eijk and de Leeuw, 1992; Wojtysiak et al., 2018). The strong winds experienced in the Arctic (e.g., in Hornsund station, the annual mean wind speed in 1978–2009 was 5.6 m s^{-1}; Marsz and Styszyńska, 2013) lead to intensive wave breaking on the sea, confirming the possibility. The most energetic sea storms have been shown to occur around Svalbard in the autumn and spring (Wojtysiak et al., 2018), and more and more open leads are forming in the Arctic Ocean in the both these seasons due to sea ice retreat (NSIDC, 2022). Currently, the Arctic is globally an area with particularly low sea spray aerosol production, likely to increase with the decreasing sea ice coverage (Jiang et al., 2021). Furthermore, sea spray has been shown to be an important transport mechanism for ionic PFAS (Per- and Polyfluoroalkyl Substances) to land in the Arctic and the Antarctic, which is consistent with more hydrophilic properties of PFAS than other POPs (Xie et al., 2022). Yet to find that the mechanism is valid for the more hydrophobic compounds, like PCBs or OCPs, would be novel if proven here.

In Svalbard, the sea spray chemical signature is observable in the local snow and rain composition (Barbaro et al., 2021) and the bulk concentration of sea salt ions decreases with distance from the sea (Koziol et al., 2021; Nawrot et al., 2016). Aerosol droplets may carry not only sea salt, but also other chemical compounds, and even bacteria (Aller et al., 2005). Such an effect may be magnified by the enrichment of pollutants in the surface microlayer of sea water, as compared to its deeper layers (e.g., Liu et al., 2014). It is rarely recognised that the surface microlayer may have a direct influence on the POPs content in surface snow on land (Casas et al., 2020; Cincinelli et al., 2005; Giannarelli et al., 2019), and it has yet to be observed whether this phenomenon occurs in the Arctic (such field observations were only made in the Antarctic, where average wind speed is higher and wave breaking more intensive than in the Arctic). As Cincinelli et al. (2005, 2001) have observed, the accumulation of hydrophobic pollutants in the surface microlayer of ocean water may increase their concentration in aerosol droplets, as may the surface processes involved in the formation of the droplets themselves (Oppo et al., 1999).

Since snow is a very efficient scavenging medium for many POPs (Lei and Wania, 2004), and it can be sampled from the ground in spatially distributed patterns (Pawlak et al., 2022), it is considered here the best sampling medium to obtain information on POPs delivery from sea spray into the terrestrial environment. Spring snow may incorporate sea spray from the highly energetic storms occurring around Svalbard (Wojtysiak et al., 2018). Furthermore, snow may form directly on sea spray particles, which are known to provide cloud condensation nuclei (as much as 90 % of cloud condensation nuclei (CCN) in marine regions can be submicron salt particles from sea spray; Clarke et al., 2006).

In this work, we hypothesise that sea spray is a an active means of dispersal for Cl-POPs in the Arctic, capable of transferring them, via snow precipitation, into the terrestrial ecosystem. We explore it through tracing correlation and co-variability of sea spray impact indices and Cl-POPs concentrations. We are aware that such an approach is not complete for confirming or negating the existence such a process, yet it provides a strong argument for or against sea spray being a secondary source of Cl-POPs. To the authors' best knowledge, this is the first study to date on the connection between the secondary emission of Cl-POPs from seawater and their deposition in snow in the Arctic.

2. Experimental

The data set used here includes samples of fresh snow and seawater collected in the vicinity of the Polish Polar Station Hornsund in two spring seasons (of 2019 and 2021). In these samples, the contents of OCPs, PCBs, metals and metalloids, as well as stable oxygen and hydrogen isotope ratios in snow and seawater were determined. These results, except for OCP and PCB content in fresh snow sampled in spring 2019 (Pawlak et al., 2022), have not been previously published.

2.1. Location

Fieldwork was conducted in the area surrounding the Polish Polar Station Hornsund, offering background environmental monitoring data and access to a varied terrain, including convenient snow and seawater sampling, and laboratory facilities for sample pre-processing. Notably, the part of Svalbard near Hornsund experiences the greatest influence of seawater component upon the chemical composition of snowfall (Barbaro et al., 2021). All samples and supporting data were collected between 12th April and 11th May 2019 and between 20th April and 14th May 2021.

Fresh snowfall was collected in seven transects (sample sets) in total (Table 1, Fig. 1). Pairs of transects 2 and 3, as well as 6 and 7, concern the same precipitation event and may be interpreted together, with caution for rapid snow aging effects.

2.2. Sampling

All snow samples were collected with a stainless steel density cutter with 1 L volume, pre-rinsed with deionised water and HPLC quality methanol, into pre-cleaned PTFE bags (approx. 6 L, Welch Fluorocarbon; triple-rinsed with MilliQ water and triple-rinsed with HPLC methanol). Sampling personnel was wearing powderfree gloves and face-masks to prevent contamination from their bodies entering the samples. More details on the snow sampling protocol in 2019 may be found in Pawlak et al. (2022) and this work has guided improvements in the snow sampling protocol for Cl-POPs in 2021 (see Supplementary Information).

Table 1
Sampling transects included in this study. Abbreviations: Cl-POPs - chlorinated persistent organic pollutants, Me – metals and metalloids, Iso – H & O stable isotopes in water.

Sample type	Transect	Date of sampling	Sampling point symbols in Fig. 1 (n sites + n extra samples from local repeats)	Types of samples collected
Fresh snow	(1) Fugleberget slope	13th April 2019	F03-F07 (5)	Cl-POPs
	(2) Revdalen (non-glaciated valley centre line)	22nd April 2019	R1-R11 (6 + 2)	Cl-POPs, Me, (Iso, $n = 4$[b])
	(3) Hans glacier approximate centre line	23rd/24th April 2019	H1–11 (11 + 2)	Cl-POPs, Me,
	(4) Hans glacier approximate centre line	10th May 2019	H1–11 (9)	Cl-POPs, Me, (Iso, $n = 8$[b])
	(5) Werenskiöld glacier along two centre lines + two additional small glaciers	21st April 2021	W1–8, TUV & FG (10)	Cl-POPs, Me, Iso
	(6) Arie glacier and Revdalen	25th April 2021	A1–2, Rx1–2 (4)	Cl-POPs, Me, Iso
	(7) Vestre Torrell and Profil glaciers, and the valley Dunderdalen	26th April 2021	DUN1–3, Pro1, VT1 (5)	Cl-POPs, Me, Iso
Surface seawater	(1) Isbjørnhamna Bay transect, where Hans glacier is terminating	18th April 2019	M1, M4, M6 & M8 (4)	Cl-POPs
	(2) Isbjørnhamna	26th April 2019	M4, M6 & M8 (3)[a]	Cl-POPs
	(3) Isbjørnhamna	10th May 2019	M1, M4, M6 & M8 (4)	Cl-POPs
	(4) Isbjørnhamna, Hansbukta[c]	4th May 2021	M1, M4, M6, M8 and M13 (5)	Cl-POPs, Me

Table footnotes:
[a] The day with 3-point collection was due to rough sea conditions preventing the collection of the sample in the open Hornsund fjord (M1).
[b] $\delta^{18}O$ and $\delta^{2}H$ were determined in selected samples from 2019 to clear doubts related to wind action following these precipitation events and the event origin.
[c] In the 2021 seawater transect, the sea surface microlayer (SSML) was also sampled.

Snow samples were stored frozen since collection, then melted in room temperature surroundings and transferred into pre-cleaned amber glass bottles (2.5 L, pre-cleaning procedure the same as for PTFE bags). Each liquid sample was preserved with 5 mL methanol per 1-kg sample and acidified to pH = 2.0 with hydrochloric acid (a sample preparation and preservation step following EPA Method 525.2). Following that, samples were stored in +4 °C until analysis.

We also collected seawater samples (Table 1, Fig. 1) into such bottles (by similarly gloved hands), and subjected them to the same preservation and storage procedures. In 2019, surface seawater (from approximately 5 cm under the surface) was collected from a hard plastic or inflatable boat (in 2019 and 2021, respectively) with a gasoline engine. The sea surface microlayer was collected using a glass plane of approx. 7000 cm^2 surface area, submerged into the sea from a drifting boat (engine switched

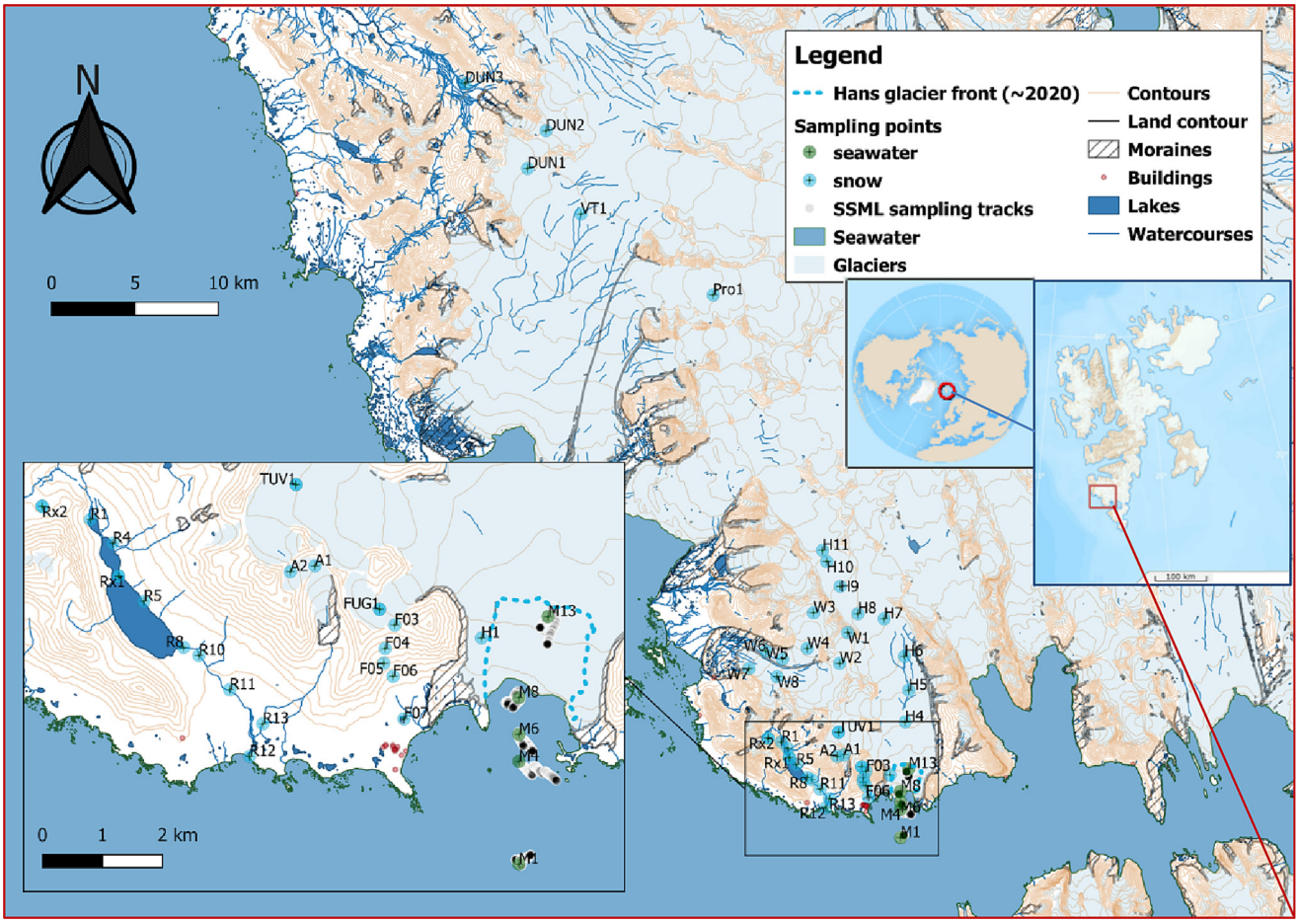

Fig. 1. Location of all sampling points, in 2019 and 2021. Please note that most locations have been sampled in only one of the years (details provided in text).
Base map source: Norwegian Polar Institute. Glacier extent may be significantly different from the current state (being up-to-date for the year 2011). To illustrate this is in the seawater collection area, the approximate position of Hans glacier front in the year 2020 has been drawn.

off during sampling) to collect a film of seawater adhering to the glass surface. According to literature, such microlayer thickness is approx. 30–50 μm (Stolle et al., 2011) or 60–100 μm (Harvey and Burzell, 1972). In our study, we have estimated the layer thickness from the collected sample volumes to be between 30 and 80 μm. The collected sample was transferred into an amber glass bottle described before with a pre-cleaned stainless-steel funnel and a pre-cleaned Teflon-coated tube.

Additional snow samples and seawater were collected for supporting information on the metal and metalloid concentration and stable isotope ratios of water, in order to track the origin of the precipitation water, the precipitation event fate and the resulting chemical admixtures (Table 1). Metal and metalloid composition was determined in samples collected into plastic cups of 50 mL volume, directly into the cup from the surface snow layer. Samples were then melted and divided into aliquots for both analyses. From seawater, a 250 mL sample bottle was collected for all additional analyses, and an aliquot of 50 mL was separated into a plastic cup for metals and metalloids analysis. All these samples were stored and transported frozen (−18 °C) until analysis. Before analysis, they were defrosted, and metal and metalloid samples were acidified with 1 % HNO_3 Suprapur (Merck).

Stable isotope samples were collected as the first samples on site to avoid contact with any methanol-cleaned equipment, mentioned earlier, which could disrupt analysis. Snow was collected directly into airtight plastic screw-top cups, and melted in the fridge upon return to the Polish Polar Station Hornsund. After a short time, allowing snow crystals in the screw of the cup to melt, the tops were tightened. Once melted, samples were immediately transferred into 4–15 mL airtight HDPE bottles (Nalgene), with no headspace. Tightly sealed bottles were then stored in +4 °C until analysis in Poland.

2.3. Sample preparation and chemical analysis

Only in 2021, snow and seawater samples were filtered through a precombusted (480 °C, 24 h) glass fiber filters (0.7 μm, GFF, Whatman), hence the 2021 data concerns only dissolved phase concentrations. In order to prepare all samples for the determination of organochlorine pesticides and PCBs, solid phase extraction (SPE) was applied. Before extraction, the appropriate amounts of isotope-labelled (p,p′-DDT-^{13}C, γ-HCH ^{13}C, PCB 28 ^{13}C, and PCB 180 ^{13}C) in the amount of 10 μL at a concentration of 10 ng mL^{-1} in dichloromethane were added to the samples. For conditioning of the octadecyl SPE cartridges, 5 mL of dichloromethane, 5 mL of ethyl acetate, 10 mL of methanol, and 10 mL of deionised water were used. Next, the investigated samples were passed through the SPE sorbent at a flow rate of 5 mL min^{-1}. After loading the test sample onto the conditioned sorbent and rising the stationary phase with 3 mL of a 1:1 (*v*/v) water/methanol mixture, the SPE sorbent was dried for 10 min. Then, analytes were eluted with 10 mL ethyl acetate and 10 mL dichloromethane. The eluate was then evaporated nearly to dryness under nitrogen flow. Finally, the extract was reconstituted to 0.1 mL applying isooctane with the addition of 100 pg (o,p′-DDT-^{13}C, α-HCH ^{13}C, PCB 52 ^{13}C, and PCB 153 ^{13}C) as injection standards.

Chemical analysis of the snow and seawater samples included different analytical techniques. Technical specifications, the reagents, standards and reference materials applied in the analytical testing of collected snow and seawater samples are summarized in Table S1 (Supplementary Information). The content of different groups of compounds, such as OCPs, PCBs, metals and metalloids were determined by gas chromatography coupled with tandem mass spectrometry (GC–MS/MS), inductively coupled plasma optical emission spectrometry (ICP-OES) and inductively coupled plasma mass spectrometry (ICP-MS). Additionally, isotopic analysis of hydrogen and oxygen (δ^2H, δ^{18}O) in selected snow samples were performed in Stable Isotope Laboratory, Institute of Geological Sciences Polish Academy of Sciences in Warsaw, Poland.

2.3.1. Quality assurance/quality control (QA/QC)

All data were subjected to accurate quality control procedures. After parameter optimization, the procedures for determining target compounds in the snow and seawater samples were validated to ensure the appropriate level of quality control and quality assurance of measurements. The analytical methodology used in the determination of different compounds in various environmental matrix compositions should be validated against certified reference materials (CRMs). In this research, we used CRMs: BCR®-365 (European Commission, Joint Research Centre, PCBs in isooctane), Trace Metals ICP-Sample 1 and Trace Metals ICP-Sample 2 (Table S1, Supplementary Information). In the case of isotopic analysis of hydrogen and oxygen in snow samples, three international standards (VSMOW, GRESP and SLAP2) were used for results calculation. Additionally, isotopically labelled standards are recommended to compensate for potential errors arising from the loss of the investigated organic compounds during sample preparation step, the matrix effects as well as the instrument response variability. Therefore, appropriate isotopically labelled standards were added to the investigated samples as surrogate internal standards (Table S1, Supplementary Information). The measuring systems were calibrated by using an appropriate standard solution of OCPs, PCBs, metals and metalloids (see Table S1, Supplementary Information). Linear calibration curves were obtained by plotting the peak area against the concentration of the respective standards. Each sample was tested in triplicate. The standard solutions were prepared immediately prior to each series of measurements. The sensitivity of the used techniques was tested by injecting standard mixtures of the target compounds in the measured concentration range. The limits of detection (LODs) and the limits of quantification (LOQs) were determined based on three independent measurements of blank samples. The limit of detection values were calculated using the formula $LOD = S + 3.3\sigma$, where S is the mean value for 10 replicates, σ is the value of the standard deviation for these replicates. In turn, the LOQs were determined as three times the LODs. Moreover, field blank samples were analysed in order to assess the degree of contamination of the test samples by transport and laboratory influence. The instrumental background was checked by inserting Milli-Q water or pure solvent blanks once per every six samples. The precision of the procedures was expressed as the coefficient of variation according to the eq. $CV = SD/X \times 100$ %, where SD is the standard deviation of the concentration of analytes and X is the average concentration of the analytes. Based on the standard samples prepared by adding a certain amount of standard solutions to clean water (MilliQ passed through an SPE cartridge), the recovery values were determined for organic compounds. The recoveries for the samples obtained by GC–MS/MS ranged 60–160 % for deionised water and 68–170 for sea water (Table S2, Supplementary Information). In the case of metal and metalloid determination, analytical accuracy was checked with two certified reference materials (Trace Metals ICP-Sample 1, Trace Metals ICP-Sample 2). CRM recovery ranged from 96 % to 104 %. In turn, the results of the determination of stable isotope ratios of O and H were reported using notation in permill (‰) relative to Vienna Standard Mean Ocean Water (VSMOW) international standard. The accuracy, controlled by internal standard measurements, was better than 1 ‰ for the δ^2H determination and better than 0.08 ‰ for δ^{18}O in H_2O determination. Analytical precision was better than 1 ‰ and 0.1 ‰ for δ^2H and δ^{18}O, respectively. The mentioned validation parameters determined for the target analytes, using particular analytical procedures, are presented in Tables S2, S3 & S4 (Supplementary Information).

2.4. Statistical analysis and air mass trajectory modelling

Cluster analysis and correlation calculations were performed with Statistica 13.3 (TIBCO®) software, cluster analysis was performed with standardised (z-transformed) data, using squared Euclidean distance and Ward's method. Metals whose content was below the detection limit in at least one of the years were excluded from statistical analysis (i.e. Ag, As, B, Be, Bi, Cd, Co, Cr, Cu, Hg, Li, Mo, Ni, Se and Sr). For correlations, Spearman rank ρ was applied due to the lack of normal distribution in the dataset. For statistical manipulations related to variability measures, all values below the LOQ or LOD were replaced with one third of the LOQ or LOD value. Initial data processing was partly performed in R version 3.6.2. (including boxplots).

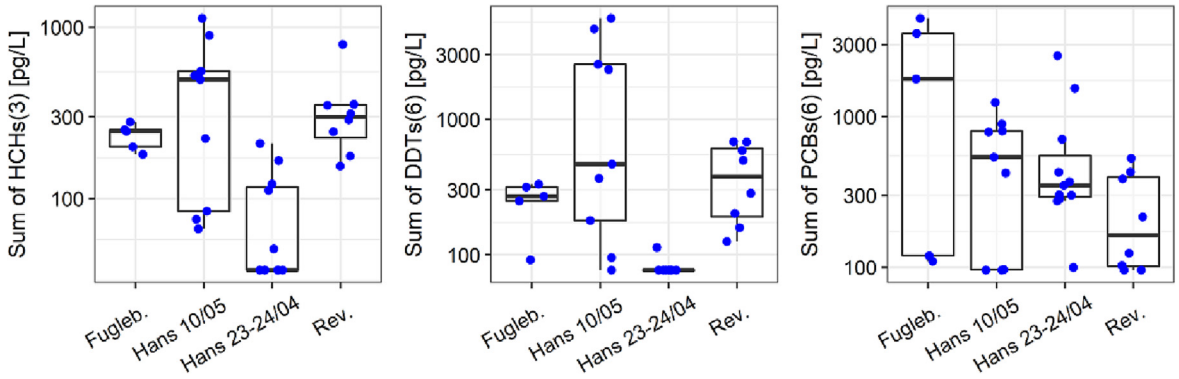

Fig. 2. Organochlorine pesticide (OCP) and polychlorinated biphenyl (PCB) contents in the snow samples collected in 2019, presented as summary parameters (the data on each compound are reported in Pawlak et al. (2022)). The box marks the Q1–Q3 span (i.e., the interquartile range [IQR]), with median marked as a thick line. Whiskers reach no further than 1.5 × IQR from the box hinge, where IQR = Q3–Q1. DDX = DDD + DDE + DDT, where: DDD = dichlorodiphenyldichloroethane; DDE = dichlorodiphenyldichloroethylene; DDT = dichlorodiphenyltrichloroethane; HCHs = hexachlorocyclohexanes. Please note the logarithmic scale of concentrations.

NOAA HYSPLIT model (Rolph et al., 2017; Stein et al., 2015) was used to plot air mass backward trajectories for each sampled precipitation event, for two elevations: a HYSPLIT-generated mid-boundary layer height and 1000 m above ground level. Eight trajectories, covering 7 h of trajectory arrivals (in hourly spacing) have been produced for each case; each trajectory extended for 72 h into the past. Mid-boundary layer height was used to simulate near-ground movement of impurity particles, including sea spray generated in the vicinity of the sampling site. The 1000 m agl is more likely to represent the low cloud cover in the area generating precipitation, as this is consistent with the prevalence of low clouds at Hornsund (Marsz and Styszyńska, 2013). However, such precipitation (up to 1.5 mm in 15 h) may also have been generated by a *Cumulus* or in the fringe of a *Cumulonimbus* cloud, hence we have checked also air mass trajectories arriving at 2000 m a.g.l.

3. Results

3.1. The content of chlorinated persistent organic pollutants (cl-POPs) in fresh snow and seawater

The content of selected organochlorine pesticides and polychlorinated biphenyls in snow from 2019 is described in Pawlak et al. (2022). The concentrations of all compounds are available in the online repository MOST Wiedzy Open Research Data Catalog (doi:10.34808/2cd8-pk41). In brief, the 2019 snow contained 160 pg L^{-1} (<LOD–1840 pg L^{-1}) ΣHCH_3, 153 pg L^{-1} (<LOD–5720 pg L^{-1}) ΣDDX and 210 pg L^{-1} (<LOD–4480 pg L^{-1}) ΣPCB_6 (medians and ranges are given; Fig. 2). In the case of snow collected in 2021, the contents of individual compounds were as follows: $\Sigma PCBs_6$ = range: <LOD–196 pg L^{-1}, median: <LOQ, where lighter PCB congeners such as PCB 28 and PCB 118 were determined only in single samples and mainly the content of heavier PCBs such as PCB 138, PCB 169 and PCB 180 was determined; ΣHCH_3 = range: <LOD–260 pg L^{-1}, median: <LOD, where α-HCH and γ-HCH were determined in only three fresh snow samples; ΣDDX = range: <LOD–266 pg L^{-1}, median: <LOD, where ΣDDX refers to the sum of DDT, DDE and DDD contents, with o,p′-DDT and p,p′-DDT contributing the most to the average content. The other pesticides tested were not detected by our method. Fig. 3 shows the distribution of individual compounds, divided into three transects. The highest variability of concentrations was found in the transect from Werenskiöld glacier.

In the case of sea water collected in 2019, the contents of individual compounds were as follows: ΣPCB_6 = range: <LOD–133 pg L^{-1}, median: 6.97 pg L^{-1}, where lighter PCB congeners such as PCB 28, PCB 52, PCB 101 and PCB 118 accounted in most cases for >70 % of the overall determined content of the total PCBs; ΣHCH_3 = range 15–401 pg L^{-1}, median: 67 pg L^{-1}; ΣDDX = range: 87–2826 pg L^{-1}, median: 141 pg L^{-1}, with the largest contribution to the average content from o,p'-DDE (89 %). Of the other pesticides we tested, only HCB, mirex and heptachlor epoxide were detected in single samples. Fig. S2 (Supplementary Information) shows the distribution of individual compounds by three dates when samples were taken, from the same sampling sites.

In the case of seawater collected in 2021, the contents of individual compounds were as follows: ΣPCB_6 = range: <LOD–85.8 pg L^{-1}, median: <LOQ pg L^{-1}, where lighter PCB congeners such as PCB 28 and PCB 118 were largely below LOQ or below LOD, hence only heavier congeners such as PCBs 138, 169 and 180 are included in the sum of PCBs. PCBs 138 and 169 were determined only in single samples; ΣHCH_3 = range: <LOD–13.8 pg L^{-1}, median: <LOD pg L^{-1}; ΣDDX = range: <LOD–107 pg L^{-1}, median: 65 pg L^{-1}, of which o,p'-DDT and p,p′-DDT had the largest contribution to the average content, constituting an average of 64 % of the total content. The other pesticides tested were not detected by our method. Fig. 4 shows the distribution of individual compounds between the regular surface seawater and the sea surface microlayer (SSML), indicating enrichment of the SSML in β-HCH, o,p′-DDT, p,p′-DDT, and the heavier PCBs, especially in PCB 169. Summary parameters also indicated enrichment in the SSML.

3.2. Metal and metalloid concentrations in the collected samples

The content of 24 and 28 metals and metalloids was determined in fresh snow samples collected in 2019 and 2021, respectively. Of the 24 elements determined in the samples from 2019, two were below the detection limit (Ag and Hg); in the case of samples from 2021, 10 variables were below the detection limit (the concentrations of Ag, As, Be, Bi, Cd, Co, Cu, Hg, Mo and Ni). Furthermore, the concentrations of Cd, Co, Cr, Cu, Se, Sr were determined only in a few snow samples from 2019, similarly to Cr and Li in snow from 2021. Table S5 shows the maximum, minimum and median concentrations of metals and metalloids determined in fresh snow (Supplementary Information).

Sodium and magnesium had the largest mass percentage share in the total of all metals and metalloids. The median percentage share is 88 % and 73 % for 2019 and 2021, which may indicate a large impact of sea aerosol on the chemical composition of snow in this area. Such impact was also demonstrated by Nawrot et al. (2016) and Barbaro et al. (2021), who surveyed snowpits across Svalbard. Fig. S3 (Supplementary Information) represents the relationship between the sodium and magnesium content and the altitude and distance from the sea from which the sample was taken. For both elements, a decrease in their content was observed with increasing altitude and distance from the sea, and indeed in the total pool of results both Na and Mg (as well as Ca) correlated significantly and negatively with the distance from the sea (Spearman rank: $\rho_{Na} = -0.567$, $\rho_{Mg} = -0.312$, $\rho_{Ca} = -0.360$; $p < 0.05$). Sodium concentrations also correlated significantly with elevation (Spearman rank: $\rho_{Na} = -0.496$, $p < 0.05$). The significance of such correlations was rarely held within smaller

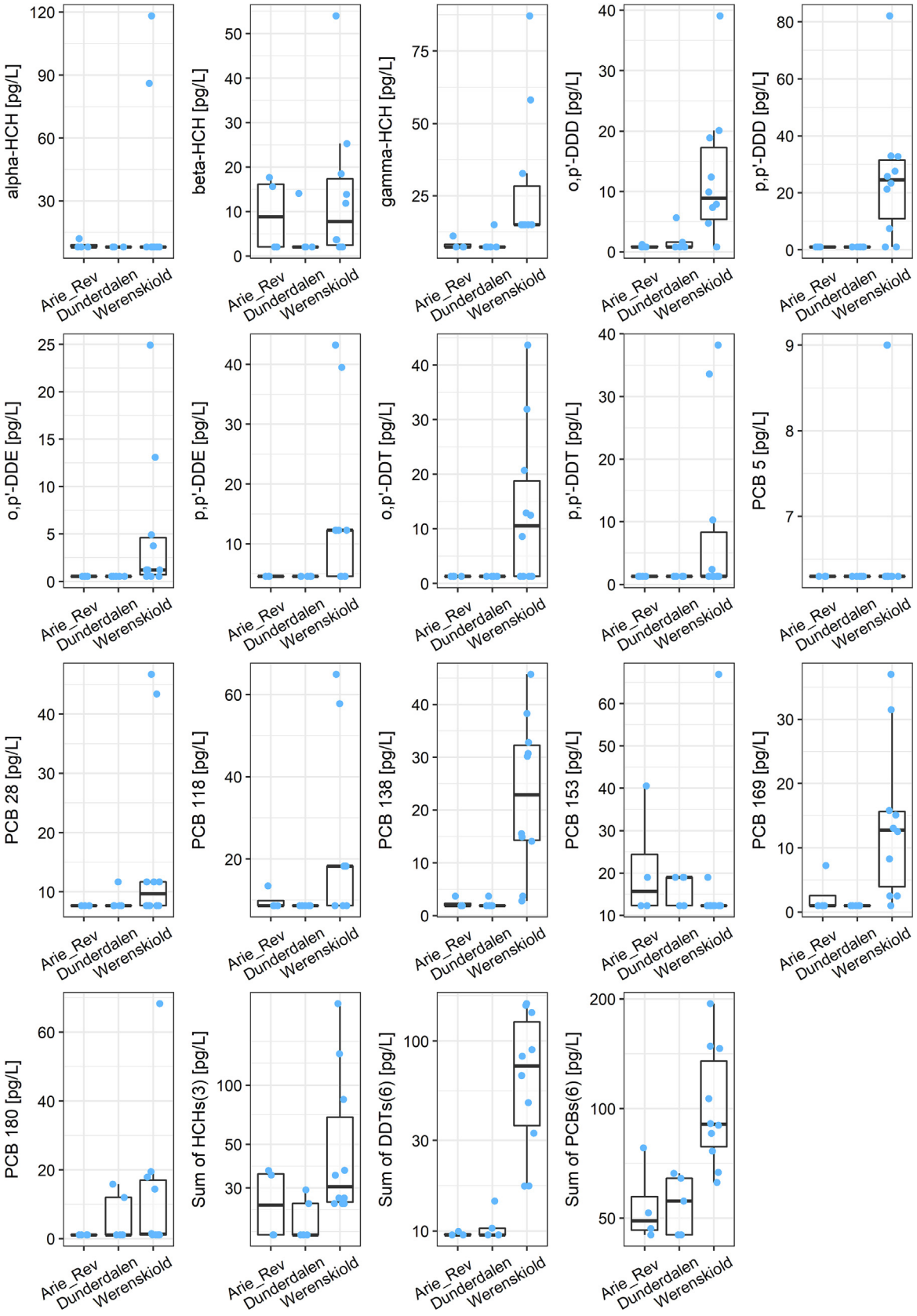

Fig. 3. Organochlorine pesticide (OCP) and polychlorinated biphenyl (PCB) contents in the snow samples collected in 2021, grouped by data series. The box marks the Q1–Q3 span (i.e., the interquartile range [IQR]), with median marked as a thick line. Whiskers reach no further than 1.5 × IQR from the box hinge, where IQR = Q3–Q1. DDD, dichlorodiphenyldichloroethane; DDE = dichlorodiphenyldichloroethylene; DDT = dichlorodiphenyltrichloroethane; HCH = hexachlorocyclohexane. Please note the change of scale type to logarithmic for the last panel with summary parameters.

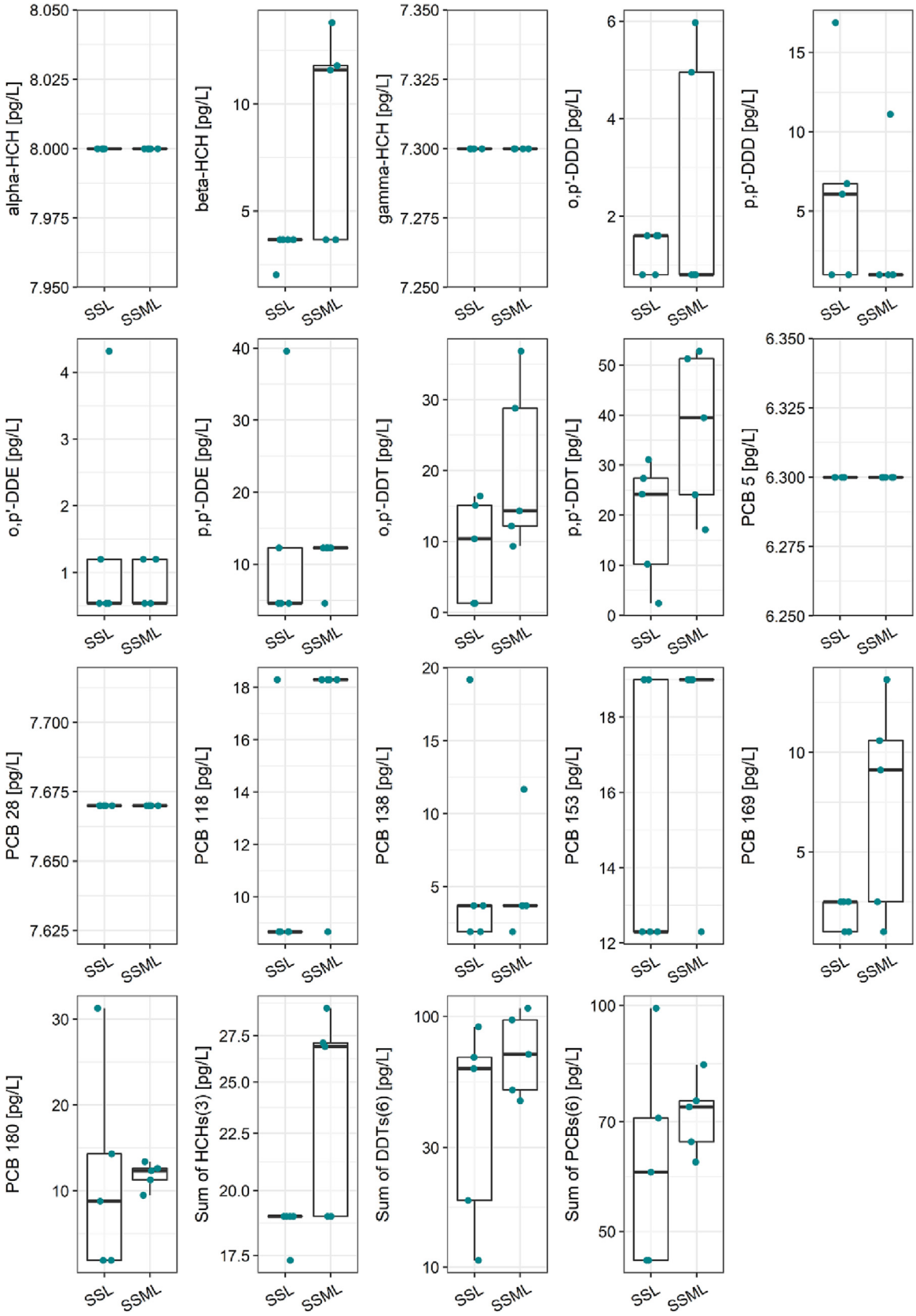

Fig. 4. Organochlorine pesticide (OCP) and polychlorinated biphenyl (PCB) contents in the sea water collected in 2021, grouped by data series. The box marks the Q1–Q3 span (i.e., the interquartile range [IQR]), with median marked as a thick line. Whiskers reach no further than 1.5 × IQR from the box hinge, where IQR = Q3–Q1. DDD = dichlorodiphenyldichloroethane; DDE = dichlorodiphenyldichloroethylene; DDT = dichlorodiphenyltrichloroethane; HCH = hexachlorocyclohexane. Please note the change of scale type to logarithmic for the last panel with summary parameters.

datasets pertaining to one precipitation event, although all such relationships were negative. They were only significant and strong for all three elements in the largest dataset from one event, i.e. the Revdalen 22nd April 2019 – Hans glacier 23rd-24th April 2019 set (Spearman rank: $\rho_{Na} = -0.767$, $\rho_{Mg} = -0.807$, $\rho_{Ca} = -0.820$; $p < 0.05$, for distance from the sea as correlated variable, and very similar coefficients for elevation). This may reflect the difficulty in interpreting small datasets and in distinguishing effects ascribed to altitude from those related to distance from the shore when sampling valleys and glaciers opening towards the sea. In addition, it was observed that the percentage of Na and Mg in the total of all metals and metalloids did not change significantly with elevation above sea level or distance from the sea.

Cluster analysis showed (Fig. 5) that in both years two clusters of metals and metalloids can be distinguished (at 72 % for 2019 and 58 % for 2021 relative distance level). Notably, the H4 point sample collected on April 23rd, 2019, was excluded from the analysis, because the metal content at this point was about ten times higher than in the other samples. For samples from 2019, we distinguished single clusters containing: 1) Ca, K, Mn, Ba, V, Mg, Na; 2) Sb, Pb, Al, Si, Fe, Zn, while in the case of samples from 2021, the clusters contained: 1) Na, Mg, K, Ca; 2) V, Fe, Al, Zn, Pb, Ba, Mn, Sb, Si. The first cluster in each case contained metals such as Na, Mg, Ca, K, which are the main cations in sea salt, suggesting that this cluster is associated with sea aerosols as their source. The second cluster contained elements such as Si, Al, Fe, which are the main components of the Earth's crust, Zn and

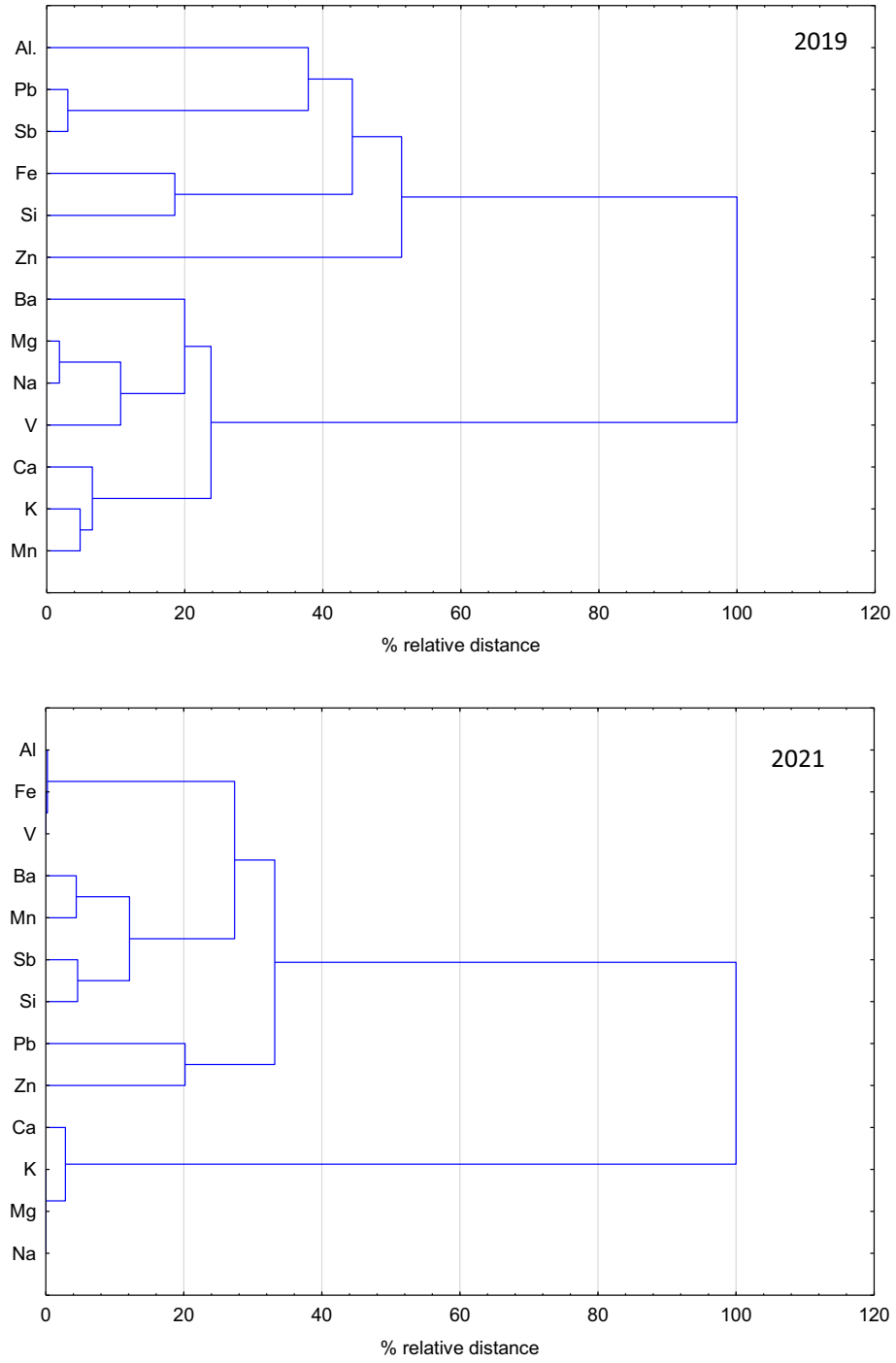

Fig. 5. Dendrogram resulting from cluster analysis of the metal and metalloid concentrations in the fresh snowfall, based on the samples collected in spring 2019 and 2021.

Sb occur in the ore-bearing veins on the western side of Hansbreen (Kieres and Piestrzyński, 1992), which means that this cluster may represent the local variability of the geological substrate. Additional contributions of long-range transport cannot be excluded, perhaps feeding the smaller differences in concentrations within each cluster. Comparing the content of Mg, Ca and K in both years, a ten-fold increase in their content was observed in 2021 compared to 2019, which may indicate that the chemical composition of snow in 2021 was more influenced by the local rock dust. Indeed, the concentrations of sodium were similar across both years and the elevated concentrations of Ca or Ca and Mg both coincided with the location of marbles or dolomites in the surfacing rocks near respective samples (please note a shift in sample locations between the years).

3.3. Stable isotope ratios in snow water

The isotopic ratios were largely different between the 2019 and 2021. 2019 snow samples (−11 to −16 ‰ in ^{18}O and −70 to −120 ‰ in ^{2}H) were significantly depleted in heavy isotopes compared to 2021 samples (−5.5 to −9.5 ‰ in ^{18}O and −35 to −55 ‰ in ^{2}H).

In 2019, the $\delta^{18}O$ and $\delta^{2}H$ values fell within a wide range, similar between the two transects where data was collected (Revdalen 22nd April and Hans glacier 10th May). The wider range of isotope ratios at Hans glacier ($\delta^{2}H = -15.45/-115.0$ to $\delta^{18}O = -6.72/-48.1$) could reflect both the wider elevation span and the possibility of including in these samples more than one snowfall event (no clear boundary was found above which to sample on May 10th upon Hans glacier). The isotopic values from 2019 were close to the world meteoric water line $\delta^{2}H = 8{\cdot}\delta^{18}O + 10$ (Craig, 1961; Fig. 6a). However, a few ratios from Hans glacier snow were below the line (especially samples H4, H5 and H6), likely indicating sublimation, since the snow was subject to wind action and may have fallen a few days prior to sample collection. We note the sublimation here as it may have also impacted the concentrations of Cl-POPs in these samples and coincided with the revolatilisation of POPs from snowpack.

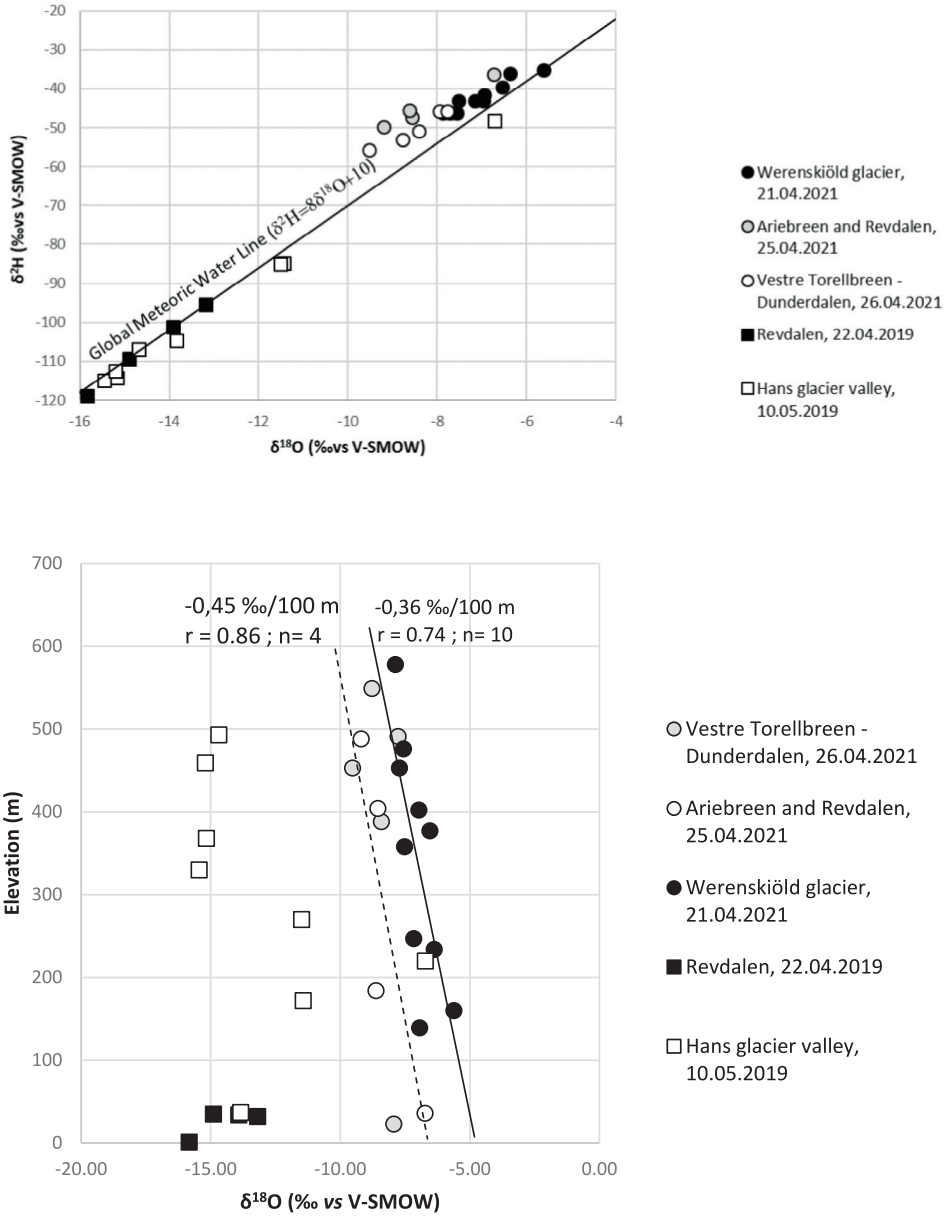

Fig. 6. Stable isotope ratios in snow water collected in 2019 and 2021 in the vicinity of Hornsund fjord: a.) the relationship between $\delta^{2}H$ and $\delta^{18}O$, including comparison to the Global Meteoric Water Line; b.) the $\delta^{18}O$ to elevation above sea level relationships, likely indicating which fresh snow was collected in situ, prior to siginificant wind redeposition.

In 2021, the isotope ratios ranged from −9.53 to −5.62 for $\delta^{18}O$ and from −55.86 to −35.17 for $\delta^{2}H$, signifying much more similar fractionation in these precipitation events across the sampled sites, supporting their origin from two snowfall events of somewhat similar characteristics. Opposite to the 2019 samples, the 2021 snowfalls fell slightly above the Global Meteoric Water Line in the $\delta^{18}O/\delta^{2}H$ graph (Fig. 6a), signifying no sublimation impact. Two distinct lines represented the 21st April and the 25th April Ariebreen and Revdalen events in the $\delta^{18}O$/elevation graph, showing rather typical elevation gradients of −0.3 to −0.4 ‰ per 100 m (Fig. 6b), and most likely only these snow events may be interpreted as the snow that fell where is was collected, i.e. without significant wind action impact. The samples collected on the 26th April showed no such clear elevation gradient, which could be due to catabatic winds shifting the snow across elevations.

The calculation of d-excess ($d = \delta^{2}H - 8 \cdot \delta^{18}O$) is a further means to demonstrate sublimation or evaporation. Any d-value below 10 indicates the remaining water or solid has undergone evaporation or sublimation. In the samples collected in 2019, several demonstrated such values (https://doi.org/10.5281/zenodo.7684167). In 2021, only the W6 sample from the 21st April event demonstrated a d-excess value below 10 (of 9.79).

3.4. POPs correlations with distance from the sea, elevation and sea salt components

The determined concentrations of single Cl-POPs and the sums of POPs categories (HCHs, DDX and PCBs) have been correlated (Spearman rank correlation) with the physical location parameters of each sample (elevation and distance from the sea shore) and with the measured concentrations of selected metals and metalloids. The main criterion of selection of both metal and metalloid and POPs concentration variables was whether in a certain dataset (or further on, a subset) the number of results exceeding LOQ has reached at least half of the number of samples (n) in the given dataset. For the entire dataset (Table S7, Supplementary Information), we found statistically significant correlations between the distance to the shore (indepedent on the method of such a measurement, whether along the valley bottom or the shortest distance across a mountain ridge) and both the α-HCH concentration and all summary parameters of POPs. All such correlations were positive, indicating higher concentrations of Cl-POPs at increasing distances from the sea; no significant altitude effect was detected. Several metals and metalloids, including the typical marine source indicator Na, correlated negatively with all the Cl-POPs sums.

When the data was split into 2019 and 2021 datasets, separately, the relationships related to physical environment persisted only for $\Sigma PCBs_5$ in 2019 (Spearman rank $\rho = 0.457$ for altitude and 0.429–0.511 for distance from the sea; $p < 0.05$). In 2019, the ΣPCBs also correlated negatively and significantly ($p < 0.05$) with the concentrations of Fe, Mg, Mn, and Si, as did PCB28 concentration with the concentrations of Fe, K, Mg and Mn. In 2021, a few elemental concentrations also correlated negatively and significantly (Spearman rank, $p < 0.05$) with the summary concentrations of Cl-POPs (Al, Ca, Mg, Pb and Si with ΣDDX and $\Sigma PCBs_5$, Mg also with ΣHCHs). Sodium was found to correlate significantly only with the concentration of ΣDDDs in 2021 ($\rho = -0.473$, $p < 0.05$). In 2019, the correlations with the physical parameters of sample location were also calculated with the inclusion of the Fugleberget trasect (snow collected on 13th April 2019, which could not be included otherwise due to lack of metal and metalloid analysis from this location), yielding the only significant Spearman rank correlation between distance from the sea and ΣDDX ($\rho = -0.387$, $p < 0.05$).

The division into single snowfall events sampled significantly reduces the *n* of the datasets analysed, yet it was necessary to explore whether any relationships can be found within a set of samples with contaminants originating from the same source (or a combination of sources, to be exact, as is usually the case with the Arctic precipitation). Selected POPs correlated significantly and usually negatively with several metals and metalloids which can be attributed to crustal sources (Al, Fe, Mn and Si, after: Koziol et al., 2021). With the elements of possibly marine origin (Na, Mg, K, Ca - Koziol et al., 2021), the significant correlations were both positive and negative. While both aforementioned relatioships occurred in both 2019 and 2021, only in 2019 did any elements of likely anthropogenic descent correlate with POPs (Sb and Pb positively in single events, Sb usually negatively with α-HCH and once with o,p′-DDT). The statistically significant correlations in single-episode datasets are summarized in the Table S8 (Supplementary Information).

3.5. Air mass backward trajectories and meteorological background of each precipitation event

The precipitation event of 12th April 2019 (1.1 mm; sampled on April 13th upon Fugleberget slope) could have originated in the south-western Svalbard and the Fram Strait or in the higher clouds arriving from the direction of Greenland across the Fram Strait (Fig. S4) (Supplementary Information). The meteorological observations at the Hornsund station reported *St neb/St fra* and *As op/Ns* in the 12 h preceding this precipitation measurement, which leads to the conclusion that precipitation occurred most likely from the *Ns* clouds, hence both the lower and higher levels of air mass backward trajectories require interpretation.

On 20th/21st April 2019 (1.3 mm solid precipitation event), the result of the lowest and higher trajectories indicated a different air mass inflow direction, from the north or the south. In the case of higher elevation trajectory, likely corresponding to the cloud level, it has crossed the Northern Atlantic, and before the coastal areas of mainland Europe, the British Isles and Iceland (Fig. 7). Again, *As op/Ns* clouds were observed during the event (when not obscured by fog), hence the higher trajectory levels have likely contributed to the precipitation composition.

The snow sampled on May 10th, 2019, was likely an accumulation of wind-blown snow from earlier precipitation events, since the last registered precipitation at the Hornsund station before that was on May 6th (with $P = 0.0$ mm, i.e. only a trace snowfall was recorded). For the likely dry deposition source in this snow, we have plotted trajectories on May 6th and 9th, and the trajectory levels (two elevations) at both dates resulted in a similar air mass inflow direction, connected to the Arctic Ocean as a source area. On the 6th May, the air has also crossed directly over Spitsbergen (Fig. S5, Supplementary Information).

In the meteorological records of Hornsund station, despite the lack of precipitation amount recorded, there are observations of weather type implying snowfall of various intensity on May 6th (at 03 UTC) and May 8th (15–00 UTC on May 9th). During the short 6th May 2019 event, the recorded clouds were *Cu fra/St fra* and *As op/Ns*; during the 8th May event, thickening *Ac* clouds were present. For this reason, we have also plotted backward trajectories on May 8th 2019, arriving at 23 UTC, at 1000 and 2000 m agl, showing a similar air inflow direction to the plots in Fig. S5 (Fig. S6; Supplementary Information).

The snowfall collected on 21st April 2021 on Werenskiöld glacier (0.5 mm, 21st April 2021), preceded by 1 mm of snow grains and freezing drizzle precipitation at Hornsund station on 20th April, has a peculiar cloud situation recorded, with *St ne* or *St fra (but not in bad weather)* and the rest of the sky obscured, which is unlikely during an ongoing precipitation event. The air mass trajectories at the time originated most likely in the Fram Strait area and the HYSPLIT model indicated precipitation connection to all tested trajectory elevation levels (Fig. 7).

Similarly, the air arriving to Hornsund fjord area on 24th April 2021 (until midnight on 25th; 0.8 mm snow fell by then) flowed over the Fram Strait, yet it crossed over the Greenland Ice Sheet before that (Fig. S8, Supplementary Information). Within the next day (data not shown), the air mass inflow direction did not change significantly, thus the same precipitation event collected on the next day should not have been impacted by a different source of dry deposition. The precipitation event recorded in the weather log at the Hornsund meteorological station lasted mainly between 06 and 21 UTC on April 24th, with a trace of snowfall produced also on April 25th, before 12UTC observation time. The event was mainly assisted by *Sc (not cumulogenitus)* clouds, occasionally by *St ne* or *St fra (but not in bad weather)* or with *Ac* showing, which could mean the precipitation

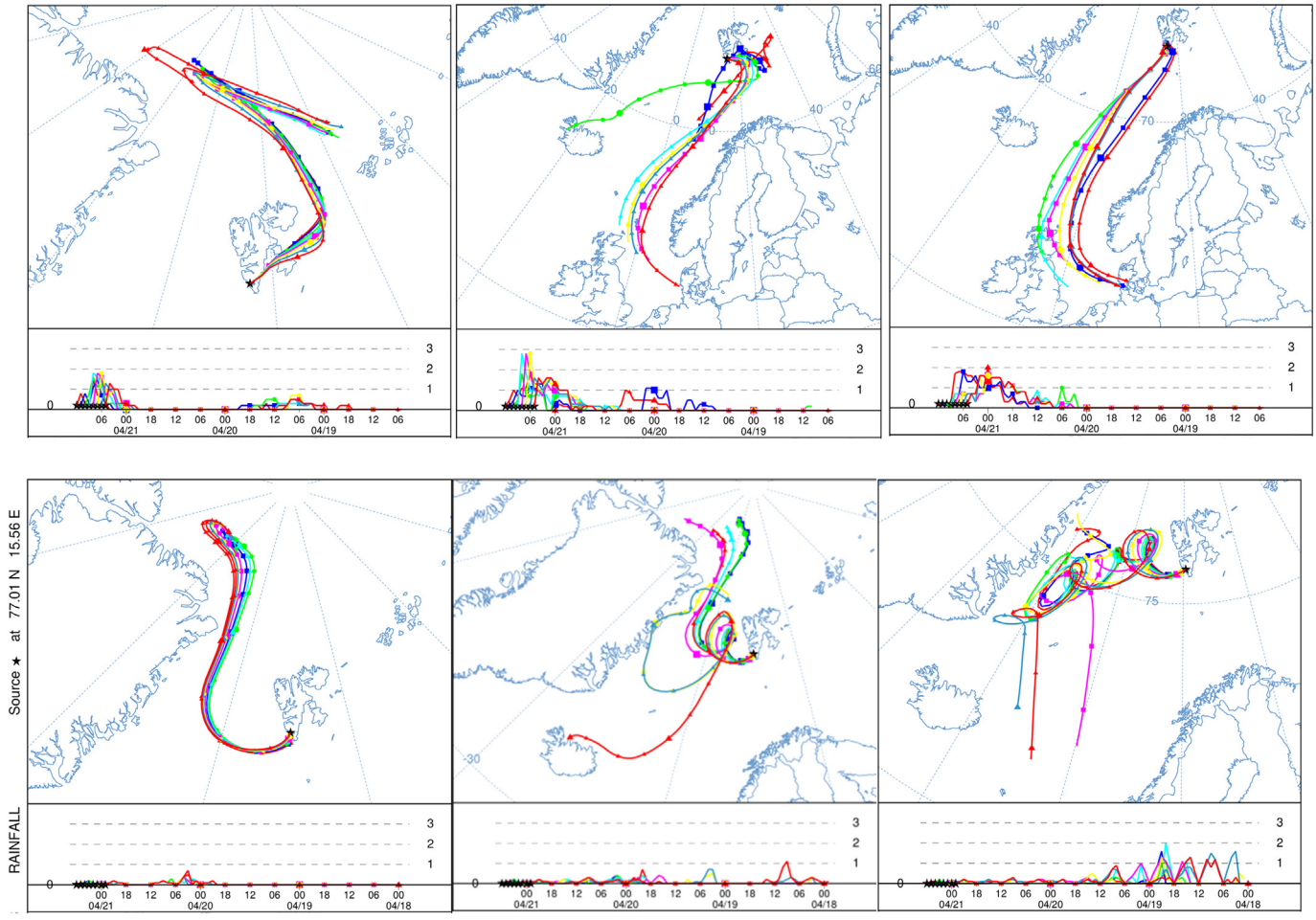

Fig. 7. Air mass trajectories arriving to Hornsund on 21 April 2019 (top row) and 21st April 2021 (bottom row), bringing snowfall events: left – automatic mid-boundary layer height, middle – 1000 m agl, right – 2000 m agl. Bottom graphs in each panel show rainfall level. Full READY HYSPLIT information is provided in Supplementary Information, Fig. S7.

originated from low clouds, yet HYSPLIT model indicated the 2000 m trajectory to have a similar contribution to precipitation at Hornsund to the lower trajectories (Fig. S8).

4. Discussion

The fresh snow sampled in the spring of 2019 was characterized by about an order of magnitude higher content of Cl-POPs than the snow collected in the spring of 2021. In addition, in 2019 the total sum of PCBs consisted mainly of more volatile congeners such as PCB 28, 52, 118, which are more susceptible to long-distance transport than heavier congeners (Gouin et al., 2004; Meijer et al., 2002), such as PCB 138, 169 and 180, which predominated in the 2021 samples. Such concentrations support the interpretation that the 2019 snowfalls were influenced by the long-range transport of Cl-POPs, while the 2021 snowfalls sampled were virtually free from its influence. This is consistent with the low aerosol concentrations in the atmospheric air at Hornsund measured by D. Kępski in 2021 (https://dataportal.igf.edu.pl/dataset/aerosol-size-distribution-0-3-10-um-at-hornsund-spring-2021/resource/962f01c1-ea9a-4a61-b498-1917194621f8).

Another argument confirming the greater impact of long-distance transport in 2019 is the origin of the air masses bringing the snowfall. Thanks to the use of retrograde trajectories of air masses, in 2019 we could distinguish air masses originating from the coasts of mainland Europe, the British Isles, Iceland and northern Russia. These are areas of much greater urbanization and unintentional emissions (cf. https://edgar.jrc.ec.europa.eu/dataset_pop60) of the compounds we determined than in the case of 2021, where the air masses came mainly from Greenland and the Fram Strait. Additionally, stable isotope ratios in snow water may be used for interpreting the moisture source of each precipitation event, yet this method is still in development and may lead to contradictory results, hence we only interpret it as a minor source of information. In 2021, the snow samples were enriched in heavier isotopes, which could mean a more southern source of moisture (Santos et al., 2020). However, interpreted together with air mass trajectories and the local differences in seawater oxygen isotope ratios within the Arctic, it is more likely that the moisture source in 2021 was connected to the warmer waters brought by the Gulf Stream into the Fram Strait (cf. LeGrande and Schmidt, 2006), and hence was closer to the shores of Svalbard than the moisture sources in 2019.

4.1. The context of the hemispheric transport of POPs in models

Seawater Cl-POPs transport models have already predicted the possibility that ocean currents act as secondary sources of Cl-POPs. Stemmler and Lammel (2013) concluded such a possibility for PCBs and DDT in waters of the North Atlantic at depths 200–1500 m. In the World Ocean, it is only a regional effect, especially present near the Gulf Stream, indicating a northward shift of pollutants (Stemmler and Lammel, 2009). However, such models reflect on deeper waters and thus do not explain the possibility of these pollutants to reemerge to the sea surface. Interestingly, surface seawater sampled by Cai et al. (2010) and analysed for the concentration of 17 OCPs, showed their total concentrations to increase northward, too, in the area of Japanese Sea, Okhotsk Sea, Bering Sea and the Arctic Ocean. The opposing spatial concentration patterns of α- and β-HCH in the snowfall

events are consistent with the interpretation of Cai et al. (2012) that α-HCH revolatilises from the northern seas, more intensively when the sea ice cover is sparse, while β-HCH is expected to be transported by ocean currents and remained undetected in the air above seawater in their study. Yang et al. (2023), while they confirm the interpretation, quantify the β-HCH concentrations in the Arctic air for ~0.02 pg m^{-3}, as opposed to ~30 ng m^{-3} in water. However, they also predict a lessening burden of β-HCH in the Arctic Ocean (due to climate change), and estimate it at 4.4–5.3 t in 2050. According to Xie et al. (2022), ocean currents and large rivers play a role in transporting multiple OCPs and PCBs (HCHs and DDTs).

Currently, POPs atmospheric deposition models which include snow (as opposed to air concentration models) are rare and subject to uncertainties in predicting actual snow concentrations of POPs, i.a. due to a multitude of processes occurring in the fresh snowpack, postdepositionally (Hansen et al., 2006), and also the difficulty in predicting particulate POPs load of the snow (Hansen et al., 2008). The spring, when we sampled snow in the Hornsund area, is also a typical period of spring maximum events in air concentrations, i.e. an intensive revolatilisation of α-HCH (and likely other POPs with low K_{OA}) from snowpack (Hansen et al., 2008). In the (UNECE, 2010) report, ocean currents and reemission from surfaces were described as important factors for the POPs fate, giving the example of β-HCH. In large-scale atmospheric transport PCBs models, according to Friedman and Selin (2016), the proximity to sources is a stronger decisive factor than temperature at the site of deposition. Therefore, the local Cl-POPs sources in the Arctic, including secondary sources, may impact the deposition in local precipitation more importantly than previously thought, by transforming far-away sources into sources of close proximity.

The future predictions of Cl-POPs atmospheric deposition in the Arctic depend on several factors, including the likely predominant emission changes (Kallenborn et al., 2012) and the varied effects of climate change, depending on the compound in question (Hansen et al., 2015; Octaviani et al., 2015). Hansen et al. (2015) reported predicted changes in the mass concentrations of 13 Cl-POPs in the water and air compartments of the Arctic, both relevant to the problem presented in this work. It is expected that α-HCH will experience a decrease of concentrations in water and an increase in the air, while β- and γ-HCH will undergo no effect for air and an increase in the water compartment. For most PCBs, only weak decrease in the water compartment will be noted (or none at all), and no effect in the air compartment. Only the compounds with the high number of chlorine atoms, such PCB180 and PCB194, shall experience decreases in both the air and water compartment. The process of Cl-POPs dispersal with sea spray may therefore change the composition of precipitation in the Arctic by enhancing the participation of compounds from the water compartment against those increasing in the air (e.g. favour the deposition of β- and γ-HCH as compared to α-HCH). This is especially of concern since, at the same time, the total mass of HCHs within the Arctic was predicted to become up to 39 % higher in the future, a much stronger effect than for PCBs (Hansen et al., 2015), and β-HCH has been described as the most bioaccumulative of the three mentioned HCH congeners (Willett et al., 1998). DDX are also predicted to be net-imported into the Arctic in the future (Octaviani et al., 2015). Of interest are also the previous predictions by Stocker et al. (2007) that Arctic seawater content of α-HCH would have been approximately 12.5 times higher in an ice-free world, signifying that sea ice acts as a barier to atmospheric pollutants entering seawater and it will gradually cease to act as one with the sea ice extent shrinking.

4.2. Factors related to the local sea spray influence

The parameter describing the influence of the sea aerosol on snow chemistry may be the content of metals of marine origin, such as sodium, magnesium, or calcium. All three mentioned elements statistically significantly negatively correlated with the distance from the sea, which shows that the aerosol impact generally decreases with the distance. Sea salt from the spray may also be important for cloud seeding. Calcium and magnesium chlorides in seawater are very important for the sea spray hygroscopicity, yet the drying of sea spray significantly reduces this property of sea aerosol (Rosati et al., 2021, 2020). Furthermore, the cloud condensation nuclei (CCN) formation from sea spray depends strongly on the temperature of water: as has been studied recently by Nielsen and Bilde (2020), each bursting bubble in the seawater produces approximately 2300 sea spray particles at 0 °C, while the respective number of particles at 19 °C is only 40. Interestingly, the experiments of Christiansen et al. (2020) exclude the role of biogenic components of the sample in CCN activity and cloud-forming potential, highlighting the role of the sea salt instead. However, sea salt and organic components of the sea spray may not behave in the same manner after emission, and thus not exhibit a linear correlation (Cincinelli et al., 2005).

For the fresh snow dataset taken in spring 2019 and 2021, we found statistically significant correlations between all summary parameters of POPs and and the distance to the sea (Table 1). Based on the literature, the phenomenon of the increase in the concentration of semi-volatile organic compounds with elevation above sea level can be explained in two ways that may occur simultaneously: The first is related to long-range transport and the process of cold condensation (Blais et al., 1998; Wang et al., 2007), and the other with the size differentiation of sea spray droplets in local transport. According to Cincinelli et al. (2005), sea spray produces various droplet sizes with an approximately equally thin surface layer enriched in organic compounds. As the aerosol droplets get smaller, which happens during their transport away from the sea, the proportion between organic compounds and sea salt in the aerosol droplets increases. Furthermore, smaller drops can be transported over longer distances, resulting in increasing concentrations of POPs in snow further away from the sea. In order to determine which of the mechanisms during our sampling was the dominant influence, the sampling years must be considered separately, as they differ significantly from each other.

In our study setting, distance from the sea (along valley bottom) covaries with the average altitude of the area surrounding a sampling point, while the altitude variable only reflects the local topography detail where each sample was collected. Therefore, an air mass approaching from the sea shore and being subject to orographic effects on precipitation is more likely to change with the general altitude of a certain area (e.g. a mountain range) than local setting (mountain peak or hollow), i.e. such changes will correlate positively with the distance from the seashore. Furthermore, it may be difficult to find a correlation between local elevation and SWE (snow water equivalent), as mountain ridges in Svalbard are frequently subject to wind action upon snowpack, and locally cornices are formed. Unsuprisingly, we did not detect a significant correlation between altitude and SWE in our dataset from the two years combined (Spearman rank $\rho = 0.09, p > 0.05$). Conversely, between the distance from the sea (along valley bottom) and SWE, the Spearman rank correlations were significant at $p < 0.05$ for both 2019 and 2021 separately and combined, achieving ρ values >0.53. Therefore, counterintuitively, we will from here on treat the "distance from the sea" variable (instead of "altitude") as a proxy for the orographic effect.

When the correlation analysis was carried out separately for data on snow samples from 2019 and 2021, the relationships related to physical environment persisted only for ΣPCBs5 in 2019 (Table S7, Supplementary Information). Additionally, in 2019 for PCB28, a negative correlation was observed for Fe, Mg, Mn, and Si, as did PCB28 concentration with the concentrations of Fe, K, Mg and Mn. These metals in 2019 were associated with an elemental concentration cluster (Fig. 5) representing metals of typically marine origin except for Fe and Si. In the case of samples from 2021, no significant correlations were found between POPs concentrations and the physical environment. However, as in the case of 2019, there were correlations between marine metals and the sums of individual POPs, which may indicate that despite the lack of a direct correlation between concentrations and the physical environment, this effect is still significant. In single transects, the correlations of Cl-POPs concentrations with crustal elements were usually negative, with marine elements both positive and negative, and with typically anthropogenic elements, significant correlations occurred only in 2019, which suggests a detachment from any single human activity source through post-emission processes. However, the connection

of Cl-POPs to the marine source is also vague and cannot be proven through the correlation analysis of metals and metalloids with Cl-POPs.

A further aspect is the seawater composition of Cl-POPs and its possible contribution to the impurities content in fresh snow. In snow, in 2019 the total consisted mainly of α-HCH and γ-HCH, while in 2021 it was mainly β-HCH and γ-HCH, where β-HCH can be transported over long distances by sea water (Yang et al., 2023). This is consistent with the classification of POPs by Wania (2006), where HCH would be classified as a "swimmer" for its long-range transport behaviour; PCBs and DDTs are generally classified as hoppers, which means that part of their transport from lower latitudes also happens in the seawater.

Similar to snow, seawater was observed to contain an order of magnitude higher concentration of POPs in 2019 than in 2021. The distribution of PCBs concentrations between congeners was somewhat similar in both years. In the sea water from 2019, DDX was dominated by o,p′-DDE, which on average accounted for 89 % of the DDX sum, and in the case of 2021 it was o,p′-DDT and p,p′-DDT, which accounted for 64 % of the DDX sum. In turn, HCHs in 2021 were represented only by β-HCH, and in 2019 mainly by α-HCH and γ-HCH.

In 2021, sea water was collected both from the regular surface seawater (SSL in Fig. 4) and the sea surface microlayer (SSML). β-HCH or PCB 169 were detected only in the SSML, and the remaining Cl-POPs showed higher concentrations in SSML than in SSL. Such a concentration pattern may indicate the enrichment of Cl-POPs in this layer, which has been demonstrated for PAHs in the Antartic by (Cincinelli et al., 2005). The possible influence of the SSML on the content of Cl-POPs in snow may be evidenced by the fact that in the case of snow and seawater sampled in 2021, the most frequently determined compounds in both matrices were the same, while in 2019 the greatest similarity in this respect occurs for seawater and snow sampled from Hans glacier on May 10th, 2019. On that day a 10 cm thick layer of snow was collected uniformly across the glacier, due to difficulty in finding the fresh snowfall boundary, and this layer could correspond to several snowfalls. Such an interpretation is, in fact, confirmed by the low d_{excess} values in these samples, suggesting these samples have undergone sublimation. Therefore, the sea aerosol could have been affecting this set of snow samples for a long time. In addition, higher concentrations of metals of typically marine origin were determined in this snow, possibly indicating a longer duration of marine aerosol dry deposition. Such an interpretation is also a way to explain the stark contrast between the higher sea aerosol impact on this snow visible in the metal composition and the fact that in 2019, sea storms, a likely source of increased sea salt emission into the nearby atmosphere, occurred within two days before the sampled April events, while preceding the May 2019 event, the seas were calm in the area (Swirad et al., 2023). Another argument in favour of the impact of dry deposition on snow is the fact that pollutants from fresh snow gradually escape after the precipitation (Finizio et al., 2006; Herbert et al., 2005), and hence for the above-mentioned case we should rather observe lower concentrations of Cl-POPs than before. However, the opposite phenomenon was observed, which can be explained by the influence of dry deposition and effects of sea aerosol on Cl-POPs concentrations.

In one of the seawater samples taken on 10th May 2019, exceptionally high Cl-POPs concentrations were determined, in a sampling site closest to the glacier front. Such high Cl-POPs concentrations may be related to the remobilisation of pollutants accumulated in the melting glacier, as described for the Hornsund fjord by (Pouch et al., 2021a). Otherwise, the concentrations of PCBs in seawater determined by us are comparable to the levels of concentrations in seawater in the Hornsund fjord (Pouch et al., 2021a), Kongsfjorden (Papale et al., 2017) and northern Alaska and the Canadian Arctic (Hoekstra et al., 2002). However, they were higher than in seawater from the Barents Sea and the North Pole area (Gustafsson et al., 2005), and the Arctic Ocean generally (Carrizo and Gustafsson, 2011), which is consistent with the likely origin of Cl-POPs in the Gulf Stream waters, as suggested by the isotopic source-tracing of snowfall. In the case of HCH, our concentration levels are comparable to those found off the coast of Greenland (Bigot et al., 2017), in the Bering Sea and the Chukchi Sea (Yao et al., 2003), slightly higher than in the North Atlantic (Lohmann et al., 2009) yet lower than in northern Alaska and the Canadian Arctic (Hoekstra et al., 2002). The exceptionally high concentrations of DDX determined by us outmatched those determined for the coasts of Greenland (Bigot et al., 2017), North Atlantic (Lohmann et al., 2009), Arctic shelf seas (Carrizo et al., 2017) or northern Alaska and the Canadian Arctic (Hoekstra et al., 2002). However, they were still within the same order of magnitude (except one outlier) as the literature-reported data, and the literature shows that DDX concentrations in the Arctic Shelf Seas are highly variable (Carrizo et al., 2017).

4.3. Is the sea spray a potential secondary source of OCPs and PCBs for the terrestrial Arctic?

While the correlations of Cl-POPs with metal and metalloid concentrations in snow, and the distance from the sea, do not yield conclusive information on whether the sea spray is locally a source of Cl-POPs delivered to land in the Arctic snow, such information does not contradict such a hypothesis, either. Therefore, we turned to a holistic analysis of all circumstances of the precipitation events sampled, and we determined a wide range of factors, from stable isotopic ratios in snow water, through sea surface microlayer Cl-POPs composition as a potential source composition, to the air mass backward trajectories and further meteorological factors forming each event. We draw a general conclusion from these circumstances that the precipitation events sampled in 2021 represent the influence of local factors, and the snow sampled on 21st and 25th April 2021 represent mainly in situ wet deposition of Cl-POPs. The composition of Cl-POPs in these precipitation events, especially on the Werenskiöld glacier, which is directly exposed to the Greenland Sea, matched closely the composition of Cl-POPs enriched in the sea surface microlayer, which is a source of spray droplets. Such a composition is largely different from the typical predominance of lighter congeners from long-range atmospheric transport or revolatilisation from sea water. Therefore we conclude that sea spray was likely a predominant source especially in the 21st April 2021 snowfall event on the Werenskiöld glacier.

If the 21st April 2021 event is interpreted so, then the deposition fluxes of Cl-POPs enriched in the SSML may be estimated based on the concentrations of such compounds in snow and the SWE of this precipitation event at each site. Such point fluxes were estimated at 0.029–0.273, 0.015–0.297, 0.006–0.090, 0.037–0.421 and 0.005 (<LOQ) – 0.348 ng m^{-2} for β-HCH, o,p′-DDT, p,p′-DDT, PCB118 and PCB169, respectively (ranges of single point values where each compound was detected). As noted before (Pawlak et al., 2022), the spatial variability in POPs concentrations across one glacier may be relatively high, and values <LOD are an interpretation challenge. Also in the event of 21st April 2021, several point concentrations fell below LOD and they served as comparison here for an interpretation of Cl-POPs fluxes which would result from such values. With our assumption of data distribution, which approximates the average concentration of all undetected POPs at the level of 1/3 LOD, such negligible fluxes may be estimated as 0.004–0.073, 0.003–0.018, 0.002–0.030, 0.010–0.117 and 0.005 – (0.033 < LOQ) ng m^{-2} for β-HCH, o,p′-DDT, p,p′-DDT, PCB118 and PCB169, respectively, during the same precipitation event. Therefore, the fluxes contributed by the sea spray are estimated here as fully detectable, yet much smaller than fluxes contributed if an event is under the influence of long-range atmospheric transport of Cl-POPs.

5. Conclusions

In this work, we hypothesized that sea aerosol is a pathway of re-emission of chlorinated persistent organic pollutants (Cl-POPs) from the marine environment, bringing these pollutants into the terrestrial ecosystem through snow precipitation. The validity of this hypothesis lies in the confirmation of several dependencies. In the microlayer of seawater, the content of Cl-POPs is enriched in relation to the ordinary surface seawater. The concentration of Cl-POPs in fresh snow correlates positively with the distance from the sea, yet the relationship itself does not resolve whether the transport mechanism of Cl-POPs is long-distance atmospheric transport

or re-emission in the sea spray, due to such distance correlating with broader area elevation in Svalbard. However, when appropriate conditions occur, such as on April 21st, 2021, when air masses came from above the Fram Strait, then the direct impact of long-range atmospheric transport can be excluded. It is then possible to determine the deposition fluxes associated with marine aerosol. Such an origin of Cl-POPs is confirmed by the snow and seawater samples taken in 2021 having a similar congener profile, especially with respect to the Cl-POPs concentrations found in the seawater microlayer. In 2019, the greatest similarity with seawater was shown for one snow transect, which most likely represented several older snowfalls, impacted by dry deposition. In the study area, such dry deposition also includes a sea spray influence. Considering that the concentration levels of some of the POPs, e.g. β-HCH and γ-HCH, will increase in the following years in seawater, it is worth exploring the topic further. When the sea spray factor is better quantified through field and laboratory research, it could be tested in atmospheric deposition models, which despite their usefulness still suffer from higher uncertainty factors than atmospheric transport models.

CRediT authorship contribution statement

Filip Pawlak: Conceptualization, Methodology, Validation, Formal analysis, Investigation, Writing – original draft, Data curation, Visualization, Writing – review & editing. **Krystyna Koziol:** Conceptualization, Methodology, Validation, Formal analysis, Investigation, Resources, Visualization, Writing – original draft, Project administration, Funding acquisition, Writing – review & editing. **Marcin Frankowski:** Validation, Resources, Writing – review & editing. **Łukasz Nowicki:** Validation, Resources, Writing – review & editing. **Christelle Marlin:** Investigation, Writing – original draft, Writing – review & editing. **Anna Maria Sulej-Suchomska:** Writing – original draft, Writing – review & editing. **Żaneta Polkowska:** Conceptualization, Resources, Supervision, Writing – review & editing.

Data availability

The data are openly available: https://zenodo.org/record/7684258 (all data versions at 10.5281/zenodo.7681432).

Declaration of competing interest

The authors declare the following financial interests/personal relationships which may be considered as potential competing interests: Krystyna Koziol reports financial support was provided by National Science Centre Poland. Filip Pawlak reports financial support was provided by National Science Centre Poland.

Acknowledgements

This study was funded by the National Science Centre, Poland project no. NCN 2017/26/D/ST10/00630, RiS ID 11108. The staff of the Institute of Geophysics PAS and the Polish Polar Station Hornsund (PPSH) are thanked for establishing and maintaining the meteorological monitoring and support during fieldwork; and so is the support from the Polish Ministry of Education and Science Project No. DIR/WK/201805 for the PPSH. Invaluable help during fieldwork was lent especially by K. Jankowska and T. Jankowski, M. Niedbalski, M. Piotrowski, K. Ziemba, T. Biernacka, K. Kosek and D. Kępski. The authors gratefully acknowledge the NOAA Air Resources Laboratory (ARL) for the provision of the HYSPLIT transport and dispersion model and/or READY website (https://www.ready.noaa.gov) used in this publication. Tõnu Martma kindly advised us on water stable isotope sampling.

Appendix A. Supplementary data

Supplementary data to this article can be found online at https://doi.org/10.1016/j.scitotenv.2023.164357.

References

Ademollo, N., Spataro, F., Rauseo, J., Pescatore, T., Fattorini, N., Valsecchi, S., Polesello, S., Patrolecco, L., 2021. Occurrence, distribution and pollution pattern of legacy and emerging organic pollutants in surface water of the Kongsfjorden (Svalbard, Norway): environmental contamination, seasonal trend and climate change. Mar. Pollut. Bull. 163. https://doi.org/10.1016/j.marpolbul.2020.111900.

Aller, J.Y., Kuznetsova, M.R., Jahns, C.J., Kemp, P.F., 2005. The sea surface microlayer as a source of viral and bacterial enrichment in marine aerosols. J. Aerosol Sci. 36, 801–812. https://doi.org/10.1016/j.jaerosci.2004.10.012.

Barbaro, E., Koziol, K., Björkman, M.P., Vega, C.P., Zdanowicz, C., Martma, T., Gallet, J.-C., Kępski, D., Larose, C., Luks, B., Tolle, F., Schuler, T.V., Uszczyk, A., Spolaor, A., 2021. Measurement report: spatial variations in ionic chemistry and water-stable isotopes in the snowpack on glaciers across Svalbard during the 2015–2016 snow accumulation season. Atmos. Chem. Phys. 21, 3163–3180. https://doi.org/10.5194/acp-21-3163-2021.

Bigot, M., Hawker, D.W., Cropp, R., Muir, D.C.G., Jensen, B., Bossi, R., Nash, S.M.B., 2017. Spring melt and the redistribution of organochlorine pesticides in the sea-ice environment: a comparative study between Arctic and Antarctic regions. Environ. Sci. Technol. 51, 8944–8952. https://doi.org/10.1021/acs.est.7b02481.

Blais, J.M., Schindler, D.W., Muir, D.C.G., Kimpe, L.E., Donald, D.B., Rosenberg, B., 1998. Accumulation of persistent organochlorine compounds in mountains of western Canada. Nature 395, 585–588. https://doi.org/10.1038/26944.

Cabrerizo, A., Muir, D.C.G., De Silva, A.O., Wang, X., Lamoureux, S.F., Lafrenière, M.J., 2018. Legacy and emerging persistent organic pollutants (POPs) in terrestrial compartments in the high arctic: sorption and secondary sources. Environ. Sci. Technol. 52, 14187–14197. https://doi.org/10.1021/acs.est.8b05011.

Cai, M.G., Qiu, C.R., Shen, Y., Cai, M.H., Huang, S.Y., Qian, B.H., Sun, J.H., Liu, X.Y., 2010. Concentration and distribution of 17 organochlorine pesticides (OCPs) in seawater from the Japan Sea northward to the Arctic Ocean. Sci. China Chem. 53, 1033–1047. https://doi.org/10.1007/s11426-010-0182-0.

Cai, M., Ma, Y., Xie, Z., Zhong, G., Möller, A., Yang, H., Sturm, R., He, J., Ebinghaus, R., Meng, X.Z., 2012. Distribution and air-sea exchange of organochlorine pesticides in the North Pacific and the Arctic. J. Geophys. Res. Atmos. 117, 1–9. https://doi.org/10.1029/2011JD016910.

Carlsson, P., Christensen, J.H., Borgå, K., Kallenborn, R., Aspmo Pfaffhuber, K., Odland, J.Ø., Reiersen, L.-O., Pawlak, J.F., 2016. AMAP 2016. Influence of Climate Change on Transport, Levels, and Effects of Contaminants in Northern Areas - Part 2.

Carrizo, D., Gustafsson, Ö., 2011. Distribution and inventories of polychlorinated biphenyls in the polar mixed layer of seven Pan-Arctic shelf seas and the interior basins. Environ. Sci. Technol. 45, 1420–1427. https://doi.org/10.1021/es103542f.

Carrizo, D., Sobek, A., Salvadó, J.A., Gustafsson, Ö., 2017. Spatial distributions of DDTs in the water masses of the Arctic Ocean. Environ. Sci. Technol. 51, 7913–7919. https://doi.org/10.1021/acs.est.7b01369.

Casas, G., Martínez-Varela, A., Roscales, J.L., Vila-Costa, M., Dachs, J., Jiménez, B., 2020. Enrichment of perfluoroalkyl substances in the sea-surface microlayer and sea-spray aerosols in the Southern Ocean. Environ. Pollut. 267. https://doi.org/10.1016/j.envpol.2020.115512.

Christiansen, S., Ickes, L., Bulatovic, I., Leck, C., Salter, M.E., Ekman, A.M.L., Bilde, M., 2020. Influence of Arctic Microlayers and Algal Cultures on Sea Spray Hygroscopicity and the Possible Implications for Mixed-phase Clouds. https://doi.org/10.1029/2020JD032808.

Cincinelli, A., Stortini, A.M., Perugini, M., Checchini, L., Lepri, L., 2001. Organic pollutants in sea-surface microlayer and aerosol in the coastal environment of Leghorn - (Tyrrhenian Sea). Mar. Chem. 76, 77–98.

Cincinelli, A., Stortini, A.M., Checchini, L., Martellini, T., Del Bubba, M., Lepri, L., 2005. Enrichment of organic pollutants in the sea surface microlayer (SML) at Terra Nova Bay, Antarctica: influence of SML on superficial snow composition. J. Environ. Monit. 7, 1305–1312. https://doi.org/10.1039/b507321a.

Clarke, A.D., Owens, S.R., Zhou, J., 2006. An ultrafine sea-salt flux from breaking waves: implications for cloud condensation nuclei in the remote marine atmosphere. J. Geophys. Res. Atmos. 111, 1–14. https://doi.org/10.1029/2005JD006565.

Craig, H., 1961. Isotopic variations in meteoric waters. Science (80-.) 133, 1702–1703. https://doi.org/10.1126/science.133.3465.1702.

Finizio, A., Villa, S., Raffaele, F., Vighi, M., 2006. Variation of POP concentrations in freshfallen snow and air on an Alpine glacier (Monte Rosa). Ecotoxicol. Environ. Saf. 63, 25–32. https://doi.org/10.1016/j.ecoenv.2005.05.004.

Friedman, C.L., Selin, N.E., 2016. PCBs in the Arctic atmosphere: determining important driving forces using a global atmospheric transport model. Atmos. Chem. Phys. 16, 3433–3448. https://doi.org/10.5194/acp-16-3433-2016.

Giannarelli, S., Onor, M., Abete, C., Termine, M., Fuoco, R., 2019. Effect of altitude and distance from the sea on fractionation processes of Persistent Organic Pollutants (POPs)associated to atmospheric aerosol from Ross Sea to Dome C, Antarctica. Microchem. J. 149. https://doi.org/10.1016/j.microc.2019.05.012.

Gouin, T., Mackay, D., Jones, K.C., Harner, T., Meijer, S.N., 2004. Evidence for the "grasshopper" effect and fractionation during long-range atmospheric transport of organic contaminants. Environ. Pollut. 128, 139–148. https://doi.org/10.1016/j.envpol.2003.08.025.

Gustafsson, Ö., Andersson, P., Axelman, J., Bucheli, T.D., Kömp, P., McLachlan, M.S., Sobek, A., Thörngren, J.O., 2005. Observations of the PCB distribution within and in-between ice, snow, ice-rafted debris, ice-interstitial water, and seawater in the Barents Sea marginal ice zone and the North Pole area. Sci. Total Environ. 342, 261–279. https://doi.org/10.1016/j.scitotenv.2004.12.044.

Hansen, K.M., Halsall, C.J., Christensen, J.H., 2006. A dynamic model to study the exchange of gas-phase POPs between air and a seasonal snowpack. Environ. Sci. Technol. 40, 2644–2652. https://doi.org/10.1021/es051685b.

Hansen, K.M., Halsall, C.J., Christensen, J.H., Brandt, J., Frohn, L.M., Geels, C., Skjøth, C.A., 2008. The role of the snowpack on the fate of alpha-HCH in an atmospheric chemistry-transport model. Environ. Sci. Technol. 42, 2943–2948. https://doi.org/10.1021/es7030328.

Hansen, K.M., Christensen, J.H., Brandt, J., 2014. The Effect of Climate Changes Versus Emission Changes on Future Atmospheric Levels of POPs and Hg in the Arctic.
Hansen, K.M., Christensen, J.H., Geels, C., Silver, J.D., Brandt, J., 2015. Modelling the impact of climate change on the atmospheric transport and the fate of persistent organic pollutants in the Arctic. Atmos. Chem. Phys. 15, 6549–6559. https://doi.org/10.5194/acp-15-6549-2015.
Harvey, G.W., Burzell, L.A., 1972. A simple microlayer method for small samples. Limnol. Oceanogr. https://doi.org/10.4319/lo.1972.17.1.0156.
Herbert, B.M.J., Halsall, C.J., Villa, S., Jones, K.C., Kallenborn, R., 2005. Rapid changes in PCB and OC pesticide concentrations in Arctic. Environ. Sci. Technol. 39, 2998–3005.
Hoekstra, P.F., O'Hara, T.M., Teixeira, C., Backus, S., Fisk, A.T., Muir, D.C.G., 2002. Spatial trends and bioaccumulation of organochlorine pollutants in marine zooplankton from the Alaskan and Canadian Arctic. Environ. Toxicol. Chem. 21, 575–583. https://doi.org/10.1002/ETC.5620210316.
Jantunen, L., Wong, F., Gawor, A., Kylin, H., Helm, P., Stern, G., Strachan, W., Burniston, D., Bidleman, T., 2015. 20 years of air-water gas exchange observations for pesticides in the Western Arctic Ocean. Environ. Sci. Technol. 49, 13844–13852. https://doi.org/10.1021/acs.est.5b01303.
Jiang, B., Xie, Z., Lam, P.K.S., He, P., Yue, F., Wang, L., Huang, Y., Kang, H., Yu, X., Wu, X., 2021. Spatial and temporal distribution of sea salt aerosol mass concentrations in the marine boundary layer from the Arctic to the Antarctic. J. Geophys. Res. Atmos. https://doi.org/10.1029/2020JD033892.
Kallenborn, R., Borga, K., Christensen, J.H., Dowdall, M., Evenset, A., Odland, J.Ø., Ruus, A., Aspmo Pfaffhuber, K., Pawlak, J., Reiersen, L.-O., 2011. AMAP Technical Report: Combined Effects of Selected Pollutants and Climate Change in the Arctic Environment.
Kallenborn, R., Halsall, C., Dellong, M., Carlsson, P., 2012. The influence of climate change on the global distribution and fate processes of anthropogenic persistent organic pollutants. J. Environ. Monit. 14, 2854–2869. https://doi.org/10.1039/c2em30519d.
Kieres, A., Piestrzyński, A., 1992. Ore-mineralisation of the Hecla Hoek succession (Precambrian) around Werenskioldbreen, south Spitsbergen. In: Birkenmajer, K. (Ed.), Studia Geologica Polonica. Polish Academy of Sciences, Institute of Geological Sciences, pp. 115–151.
Kosek, K., Kozioł, K., Luczkiewicz, A., Jankowska, K., Chmiel, S., Polkowska, Ż., 2019. Environmental characteristics of a tundra river system in Svalbard. Part 2: chemical stress factors. Sci. Total Environ. 653. https://doi.org/10.1016/j.scitotenv.2018.11.012.
Koziol, K., Uszczyk, A., Pawlak, F., Frankowski, M., Polkowska, Z., 2021. Seasonal and spatial differences in metal and metalloid concentrations in the snow cover of Hansbreen, Svalbard. Front. Earth Sci. 8. https://doi.org/10.3389/feart.2020.538762.
LeGrande, A.N., Schmidt, G.A., 2006. Global gridded data set of the oxygen isotopic composition in seawater. Geophys. Res. Lett. 33, 1–5. https://doi.org/10.1029/2006GL026011.
Lei, Y.D., Wania, F., 2004. Is rain or snow a more efficient scavenger of organic chemicals? Atmos. Environ. 38, 3557–3571. https://doi.org/10.1016/j.atmosenv.2004.03.039.
Liu, Q., Hu, X., Jiang, J., Zhang, J., Wu, Z., 2014. Comparison of the water quality of the surface microlayer and subsurface water in the Guangzhou segment of the Pearl River, China. J. Geogr. Sci. 24, 475–491. https://doi.org/10.1007/s11442-014-1101-7.
Lohmann, R., Gioia, R., Jones, K.C., Nizzetto, L., Temme, C., Xie, Z., Schulz-Bull, D., Hand, I., Morgan, E., Jantunen, L., 2009. Organochlorine pesticides and PAHs in the surface water and atmosphere of the North Atlantic and Arctic Ocean. Environ. Sci. Technol. 43, 5633–5639. https://doi.org/10.1021/es901229k.
Ma, J., Hung, H., Tian, C., Kallenborn, R., 2011. Revolatilization of persistent organic pollutants in the Arctic induced by climate change. Nat. Clim. Chang. 1, 255–260. https://doi.org/10.1038/nclimate1167.
Ma, J., Hung, H., Macdonald, R.W., 2016. The influence of global climate change on the environmental fate of persistent organic pollutants: a review with emphasis on the Northern Hemisphere and the Arctic as a receptor. Glob. Planet. Chang. 146, 89–108. https://doi.org/10.1016/j.gloplacha.2016.09.011.
Marsz, A.A., Styszyńska, A., 2013. Climate and Climate Change at Hornsund, Svalbard. Gdynia Maritime University, Gdynia.
McGovern, M., Borgå, K., Heimstad, E., Ruus, A., Christensen, G., Evenset, A., 2022. Small Arctic rivers transport legacy contaminants from thawing catchments to coastal areas in Kongsfjorden, Svalbard. Environ. Pollut. 304. https://doi.org/10.1016/j.envpol.2022.119191.
Meijer, S.N., Steinnes, E., Ockenden, W.A., Jones, K.C., 2002. Influence of environmental variables on the spatial distribution of PCBs in Norwegian and U.K. soils: implications for global cycling. Environ. Sci. Technol. https://doi.org/10.1021/es010322i.
Muir, D.C.G., Galarneau, E., 2021. Polycyclic aromatic compounds (PACs) in the Canadian environment: links to global change. Environ. Pollut. https://doi.org/10.1016/j.envpol.2021.116425.
Nawrot, A.P., Migała, K., Luks, B., Pakszys, P., Głowacki, P., 2016. Chemistry of snow cover and acidic snowfall during a season with a high level of air pollution on the Hans Glacier, Spitsbergen. Polar Sci. 10, 249–261. https://doi.org/10.1016/j.polar.2016.06.003.
Nielsen, L., Bilde, M., 2020. Exploring controlling factors for sea spray aerosol production: temperature, inorganic ions and organic surfactants. Tellus Ser. B Chem. Phys. Meteorol. 72, 1–10. https://doi.org/10.1080/16000889.2020.1801305.
Nilsson, E.D., Rannik, U., Swietlicki, E., Leck, C., Aalto, P.P., Zhou, J., Norman, M., 2001. Turbulent aerosol fluxes over the Arctic Ocean 2. Wind-driven sources from the sea. J. Geophys. Res. 106, 32139–32154.
NSIDC, 2022. website of the National Snow and Ice Data Center, Charctic Interactive Sea Ice Graph. https://nsidc.org/arcticseaicenews/charctic-interactive-sea-ice-graph/. (Accessed 31 December 2022).
Octaviani, M., Stemmler, I., Lammel, G., Graf, H.F., 2015. Atmospheric transport of persistent organic pollutants to and from the Arctic under present-day and future climate. Environ. Sci. Technol. 49, 3593–3602. https://doi.org/10.1021/es505636g.
Oppo, C., Bellandi, S., Innocenti, N.D., Stortini, A.M., Loglio, G., Schiavuta, E., Cini, R., 1999. Surfactant components of marine organic matter as agents for biogeochemical fractionation and pollutant transport via marine aerosols. Mar. Chem. 63, 235–253.
Papale, M., Giannarelli, S., Francesconi, S., Di Marco, G., Mikkonen, A., Conte, A., Rizzo, C., De Domenico, E., Michaud, L., Giudice, A. Lo, 2017. Enrichment, isolation and biodegradation potential of psychrotolerant polychlorinated-biphenyl degrading bacteria from the Kongsfjorden (Svalbard Islands, High Arctic Norway). Mar. Pollut. Bull. 114, 849–859. https://doi.org/10.1016/J.MARPOLBUL.2016.11.011.
Pawlak, F., Koziol, K., Polkowska, Z., 2021. Chemical hazard in glacial melt? The glacial system as a secondary source of POPs (in the Northern Hemisphere). A systematic review. Sci. Total Environ. 778, 145244. https://doi.org/10.1016/j.scitotenv.2021.145244.
Pawlak, F., Koziol, K.A., Kosek, K., Polkowska, Z., 2022. Local variability in snow concentrations of chlorinated persistent organic pollutants as a source of large uncertainty in interpreting spatial patterns at all scales. J. Environ. Qual. 51, 411–424. https://doi.org/10.1002/jeq2.20343.
Pouch, A., Zaborska, A., Mazurkiewicz, M., Winogradow, A., Pazdro, K., 2021a. PCBs, HCB and PAHs in the seawater of Arctic fjords – distribution, sources and risk assessment. Mar. Pollut. Bull. 164, 111980. https://doi.org/10.1016/J.MARPOLBUL.2021.111980.
Pouch, A., Zaborska, A., Pazdro, K., 2021b. Levels of dioxins and dioxin-like polychlorinated biphenyls in seawater from the Hornsund fjord (SW Svalbard). Mar. Pollut. Bull. 162, 111917. https://doi.org/10.1016/j.marpolbul.2020.111917.
Rolph, G., Stein, A., Stunder, B., 2017. Real-time Environmental Applications and Display sYstem: READY. Environ. Model. Softw. 95, 210–228. https://doi.org/10.1016/j.envsoft.2017.06.025.
Rosati, B., Paul, A., Iversen, E.M., Massling, A., Bilde, M., 2020. Reconciling atmospheric water uptake by hydrate forming salts. Environ Sci Process Impacts 22, 1759–1767. https://doi.org/10.1039/d0em00179a.
Rosati, B., Christiansen, S., Dinesen, A., Roldin, P., Massling, A., Nilsson, E.D., Bilde, M., 2021. The impact of atmospheric oxidation on hygroscopicity and cloud droplet activation of inorganic sea spray aerosol. Sci. Rep. 11, 1–13. https://doi.org/10.1038/s41598-021-89346-6.
Santos, E.A. dos, Evangelista, H., Valeriano, C. de M., Neto, C.C.A., Castagna, A., Heilbron, M., 2020. Origin and radiogenic isotope fingerprinting of aerosols over the Southwestern Atlantic and corresponding Southern Ocean Sector. Aeolian Res. 45, 100596. https://doi.org/10.1016/j.aeolia.2020.100596.
Stein, A.F., Draxler, R.R., Rolph, G.D., Stunder, B.J.B., Cohen, M.D., Ngan, F., 2015. NOAA's HYSPLIT atmospheric transport and dispersion modeling system. Bull. Am. Meteorol. Soc. 96, 2059–2077. https://doi.org/10.1175/BAMS-D-14-00110.1.
Stemmler, I., Lammel, G., 2009. Cycling of DDT in the global environment 1950-2002: world ocean returns the pollutant. Geophys. Res. Lett. 36, 1–5. https://doi.org/10.1029/2009GL041340.
Stemmler, I., Lammel, G., 2013. Evidence of the return of past pollution in the ocean: a model study. Geophys. Res. Lett. 40, 1373–1378. https://doi.org/10.1002/grl.50248.
Stocker, J., Scheringer, M., Wegmann, F., Hungerbühler, K., 2007. Modeling the effect of snow and ice on the global environmental fate and long-range transport potential of semivolatile organic compounds. Environ. Sci. Technol. 41, 6192–6198. https://doi.org/10.1021/es062873k.
Stolle, C., Labrenz, M., Meeske, C., Jürgens, K., 2011. Bacterioneuston community structure in the southern baltic sea and its dependence on meteorological conditions. Appl. Environ. Microbiol. 77, 3726–3733. https://doi.org/10.1128/AEM.00042-11.
Swirad, Z.M., Moskalik, M., Herman, A., 2023. Wind Wave and Water Level Dataset for Hornsund, Svalbard (2013-2021). https://doi.org/10.5194/essd-2023-21.
UNECE, 2010. Hemispheric Transport of Air Pollution 2010, Part C: Persistent Organic Pollutants. United Nations, New York and Geneva.
van Eijk, A.M.J., de Leeuw, G., 1992. Modeling aerosol particle size distributions over the North Sea. J. Geophys. Res. 97, 14417–14429. https://doi.org/10.1029/92JC01214.
Wang, F., Zhu, T., Xu, B., Kang, S., 2007. Organochlorine pesticides in fresh-fallen snow on East Rongbuk Glacier of Mt. Qomolangma (Everest). Sci. China Ser. D Earth Sci. 50, 1097–1102. https://doi.org/10.1007/s11430-007-0079-8.
Wania, F., 2006. Potential of degradable organic chemicals for absolute and relative enrichment in the Arctic. Environ. Sci. Technol. 40, 569–577.
Willett, K.L., Ulrich, E.M., Hites, R.A., 1998. Differential toxicity and environmental fates of hexachlorocyclohexane isomers. Environ. Sci. Technol. https://doi.org/10.1021/es9708530.
Wojtysiak, K., Herman, A., Moskalik, M., 2018. Wind wave climate of West Spitsbergen: seasonal variability and extreme events. Oceanologia 60, 331–343. https://doi.org/10.1016/j.oceano.2018.01.002.
Wong, F., Jantunen, L.M., Pućko, M., Papakyriakou, T., Staebler, R.M., Stern, G.A., Bidleman, T.F., 2011. Air−water exchange of anthropogenic and natural organohalogens on international polar year (IPY) expeditions in the Canadian Arctic. Environ. Sci. Technol. 45, 876–881. https://doi.org/10.1021/es1018509.
Xie, Z., Zhang, P., Wu, Z., Zhang, S., Wei, L., Mi, L., Kuester, A., Gandrass, J., Ebinghaus, R., Yang, R., Wang, Z., Mi, W., 2022. Legacy and emerging organic contaminants in the polar regions. Sci. Total Environ. 835, 155376. https://doi.org/10.1016/j.scitotenv.2022.155376.
Yang, P.F., Macdonald, R.W., Hung, H., Muir, D.C.G., Kallenborn, R., Nikolaev, A.N., Ma, W.L., Liu, L.Y., Li, Y.F., 2023. Modeling historical budget for β-Hexachlorocyclohexane (HCH) in the Arctic Ocean: a contrast to α-HCH. Environ. Sci. Ecotechnol. 14. https://doi.org/10.1016/j.ese.2022.100229.
Yao, Z., Jiang, G., Cai, Y., Xu, H., Ma, Y., 2003. Status of persistent organic pollutants and heavy metals in surface water of Arctic region. Chin. Sci. Bull. 48, 131–135. https://doi.org/10.1360/03TB9026/METRICS.